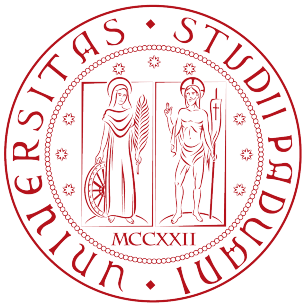

Università degli Studi di Padova

DIPARTIMENTO DI INGEGNERIA DELL'INFORMAZIONE
Corso di Laurea Magistrale in Ingegneria delle Telecomunicazioni

OTDR-based Monitoring in Passive Optical Networks

Relatore:
Ch.mo Prof. Marco Santagiustina

Laureando:
Bruno Tonello

Anno Accademico 2014-2015

Ai miei genitori.

Contents

List of Figures

List of abbreviations

AE active ethernet

AOM acousto-optic modulator

ASE amplified spontaneous emission

AWG array waveguide grating

CO central office

EAM electro-absorption modulator

EDFA erbium doped fiber amplifier

FBG fiber Bragg grating

FTTB fiber to the building

FTTC fiber to the curb (or cabinet)

FTTD fiber to the desk

FTTH fiber to the home

HSPA high speed packet access

LLU local loop unbundling

LTE long term evolution

NG-PON next generation passive optical network

ODN optical distribution network

OLT optical line termination

ONT optical network termination

ONU optical network unit

OSA optical spectrum analyzer

OTDR optical time domain reflectometer

PBF pass band filter

PG pulse generator

PON passive optical network

PS power splitter

PtP

R-SOA reflective semiconductor optical amplifier

RN remote node

SOA semiconductor optical amplifier

TDM time division multiplexing

TWDM time and wavelength division multiplexing

WDM wavelength division multiplexing

XDSL digital subscriber line technology

Chapter 1

Introduction

The recent growth of Internet traffic due to multimedia and high-interactive services has driven network operators to invest in the backbone optical networks, incrementing transmission capacity. Final users can not take advantage of this increase because the access network does not have sufficiently high capacity. In the last ten years the access network capacity has been increased thanks to new technologies as xDSL, 3G (and HSPA), and recently LTE.
Despite of these improvements, these solutions are not considered *future-proof*, and the next step is the ultra-wide band access network. One of the most promising technology, that will replace the current copper-infrastructure, is the PON (*Passive Optical Network*). Optical access networks allow future traffic support thanks to the high transmission capacity of optical fiber, and overcome the limitations of DSL and wireless systems. One of the open issues of optical networks consists in monitoring the network itself: the problem lies in identification and localization of any failure or malfunction in the links to end users, in particular because PON topology is point to multipoint, differently from backbone optical network, and because the fiber is deployed also in client premises, i.e. outside the control of telecom operators.
The purpose of this thesis is the implementation of an experimental monitoring system for passive optical netowrk using OTDR (*Optical Time-Domain Reflectometer*). In particular I focus on TDM-PON (*Time Division Multiplexing PON*), WDM-PON (*Wavelength Division Multiplexing PON*) and TWDM-PON (*Time and Wavelength Division Multiplexing PON*) proposing different monitoring schemes.
The thesis is organized as follows:

Chapter 2 Here I introduce the current access network situation and I present PON networks and the monitoring problem. I also give an

overview on OTDR-based measures.

Chapter 3 This chapter provides a description of the instrumentation and the experimental setup.

Chapter 4 The main results obtained are presented and commented. I also discuss the problems encountered during the implementation of the system.

Chapter 5 Here I present the conclusions, and I also take into consideration open issues and future developments.

Chapter 2

Optical Access Networks

The access network is the part of a telecommunication network which connects final users to their service provider, whilst the core network provides connectivity between different service providers. We can further divide the access network in two different parts: the feeder (or primary) network and the distribution (or secondary) network. The first connects the Central Office (CO) with distribution cabinet, that is connected with the final users through the distribution network. In figure 2.1 a typical access network is represented.
The Italian access network is characterized by an intensive use of copper cables and in particular of the xDSL technology. One of the most constraining element in the DSL technology is the distance between final users and central office: if the CO is located within a few kilometers, it's possible to reach a capacity of some megabits per second. The recent bandwidth request is making this technology obsolete, in favour of optical access networks.

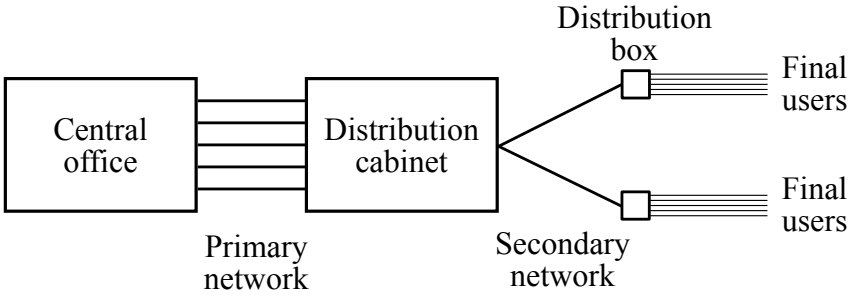

Figure 2.1: Scheme of a xDSL access network.

2.1 Passive Optical Network

Generally, there are three types of optical access networking technologies: point-to-point (PtP) fiber, active Ethernet network and passive optical network. The main differences in these three types of optical network consist in the devices installed between the central office and subscriber's terminal (or network).

Point-to-point fiber The PtP fiber architecture employs a direct fiber connection between the central office and the subscriber Optical Network Terminator (ONT). This choice has several advantages: since the fiber connection is dedicated to each user the are small loss in optical power, which allows longer distances between CO and subscriber terminal. On the contrary the elevated number of fibers impacts the size of the central office.

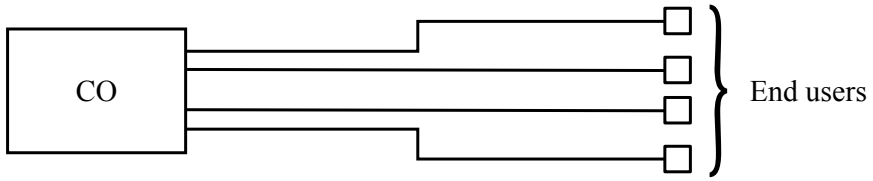

Figure 2.2: Point-to-point fiber.

Active Ethernet network This type of network exploits electrically powered devices such as switches and routers to handle different subscribers. The main differences with respect to the previous topology is the point-to-multipoint structure, which allows a considerable reduction of the number of fibers that terminate at the central office. Also in this case the distance between CO and subscribers is not a critical design issue.

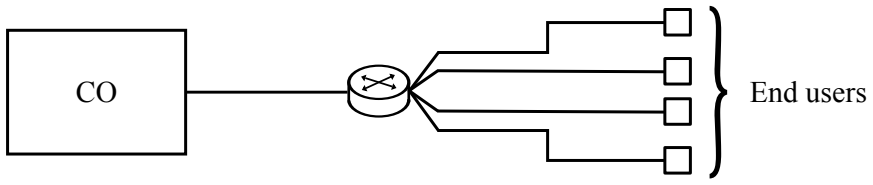

Figure 2.3: Active Ethernet network.

Passive Optical Network Similar to active Ethernet case, Passive Optical Network (PON) adopts a point-to-multipoint topology, replacing the switch with one or more passive optical components (such as power

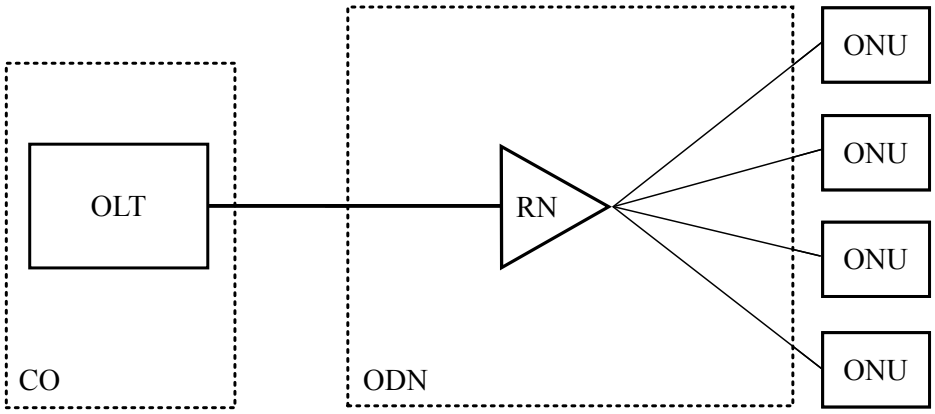

Figure 2.4: Passive Optical Network.

splitter or array wavelength gratings). The main advantages of this choice are the power consumption, the low cost of optical components (with respect to active Ethernet), the lower fiber deployment cost (with respect PtP fiber choice). Thanks to the trade-off between cost and performances passive optical networks are considered the next generation of access network.

Referring to figure 2.4, the main components of a passive optical network are:

- Optical Line Terminal (OLT): this element is the interface between the backbone network and the optical access network, it's located at the service provider central office;
- Optical Network Unit (ONU): this device is located near end users, as we will see later it could be the interface between the primary optical network and the secondary network realized with copper cables.
- Optical Distribution Network (ODN): it connects the OLT in the central office with the ONU, in other words it's the feeder network;
- Remote Node (RN): it's a passive optical component that split and combine optical signals (e.g. passive power splitter or a arrayed waveguide grating). Since the remote node is passive its cost is low, and there is no need of power supply and temperature control.

Passive optical networks can be classified with respect to the fiber penetration from the optical line terminator to the end user. Following the G.983 ITU-T recommendation I give the following definitions (figure 2.5). Several

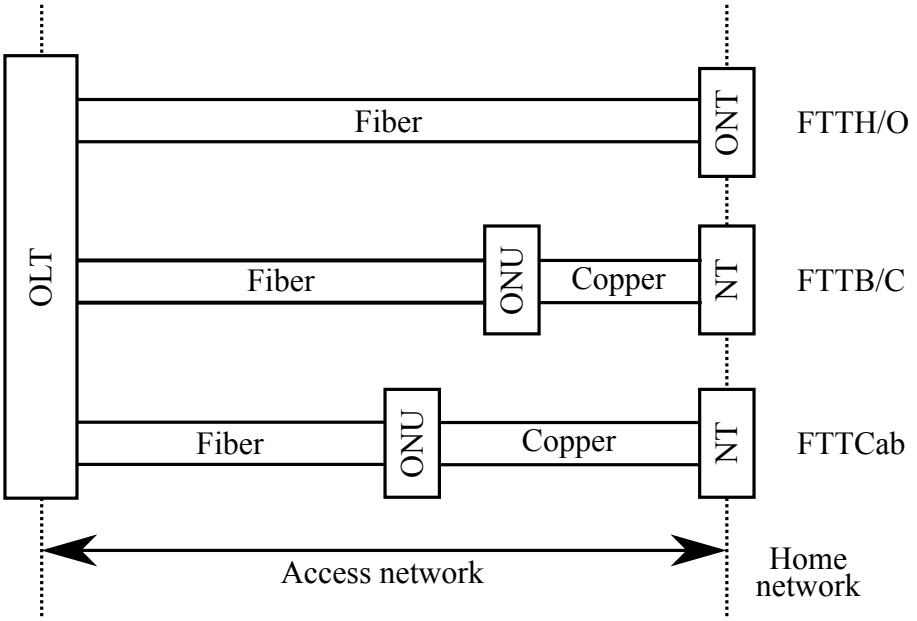

Figure 2.5: FTTx network architecture according to G.983 ITU-T recommendation.

variations can be found in literature (e.g. Fiber-To-The-Desk), here I present the three main network architectures.

Fiber To The Cabinet (FTTCab) The fiber link is terminated at a street cabinet, the distance to the subscribers is within the range of high bandwidth copper lines such as Ethernet or Wi-Fi technologies. From the cabinet to subscribers, a copper-based link is provided. FTTC is recently seen as an intermediate step towards fiber-to-the-home and it's currently used by telecom servece providers.

Fiber To The Building/Curb (FTTB/C) Similar to FTTCab the optical fiber reaches the boundary of the building and the final connection is is realized through Ethernet or Wi-Fi technologies.

Fiber To The Home/Office (FTTH/O) The fiber connection reaches directly the subscriber's home. Usually the fiber is terminated at a box on the outside wall of the house.

2.2 PON multiple access techniques

Different multiplexing schemes and architectures have been proposed in the last two decades depending on the standard. In this section, following the time evolution of PON standards, we focus on Time Division Multiple Access (TDMA), Wavelength Division Multiple Access (WDMA), and Time and Wavelength Division Multiple Access (TWDMA). I choose TWDMA instead of other proposed solutions because it has been selected in 2012 by FSAN (Full Service Access Network group) as primary solution for NG-PON2 (Next-Generation PON2).

2.2.1 TDM PON

The scheme of a TDM passive optical network is showed in figure 2.6. With a TDM scheme, the remote node is a passive power splitter and each ONU transmits and receives at the same wavelength, so they require the same optical devices.
The downstream traffic, organized in frames, is sent by the OLT to each ONU as depicted in figure 2.6. Using the timeslot, a special field in the frame format, each ONU selects from the downstream data the information of interest. A frame is delimited by a preamble, within each frame the timeslots are identified by additional preambles (at least one for each ONU). The timeslot duration can vary from a few microseconds up to some milliseconds depending on the specific protocol and on the number on ONU in the network.
As I said above, the ONUs transmit at the same wavelength and cannot communicate directly, so each ONU ignores the status of others. The access to the channel must be controlled in order to avoid collisions at the remote node, furthermore the access control must be dynamic because different ONUs could have different upload requirements. The solution is a reservation-based protocol, which requires:

- a centralized controller at the OLT;
- a signaling protocol both at the OLT and at the ONUs: the OLT queries each ONU which replies communicating its state (information to transmit), and then the OLT sends the grant for the timeslot;
- ONU synchronization (common time reference): each ONU must know exactly the beginning and the duration of its timeslot in order to avoid collision at the remote node (note that the distance between ONU and OLT is very important for a correct synchronization);

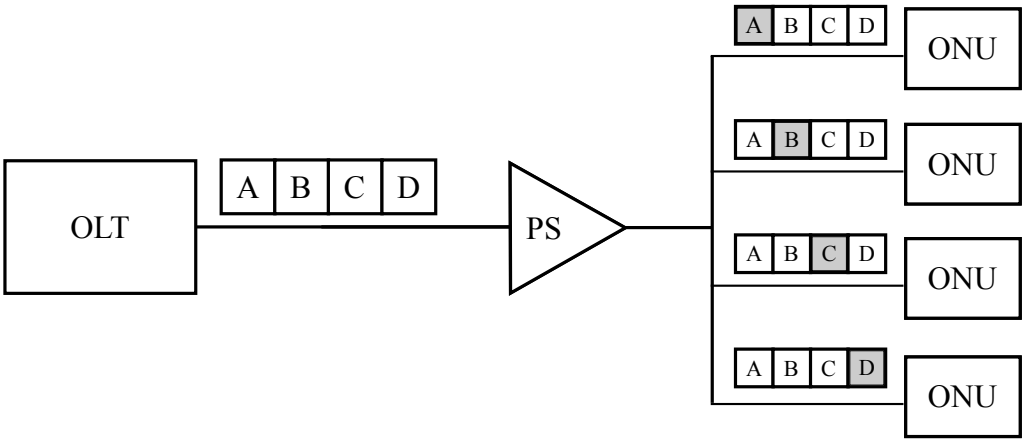

Figure 2.6: TDM PON scheme

- scheduling algorithm at the OLT: timeslots are assigned dynamically according to the state of the UNUs , the QoS requirements and the subscriber trade agreements.

The ONU receiver is simple because the received power is always the same, on the contrary the OLT receiver is more complex because the ONUs can be at different distances so it receive frames with different optical powers: it need a gain control in order to adapt the threshold between 0 and 1.

2.2.2 WDM PON

The main idea in WDM optical access network consists in supplying each subscriber with a different wavelength rather than sharing the same one between 32 (or even more) subscribers as in TDM PON. In particular each ONU transmits and receives at two different and dedicated wavelengths. The C-band is used for the upstream transmission and the L-band for the downstream.
As depicted in figure 2.7 the remote node is just an array waveguide grating (AWG) that splits and combines optical signals at different frequencies. This architecture has several advantages with respect to TDM solution: each subscriber can access to the full bandwidth accommodated by one or more dedicated wavelength, furthermore this network provides better security since each user receives only its own data. The MAC layer is simpler: first, it does not require reservation-based protocol at the remote node; second, users with different bandwidth requirements and trade agreements can be managed independently.
The complexity of the OLT and ONU transmitters and receivers is higher

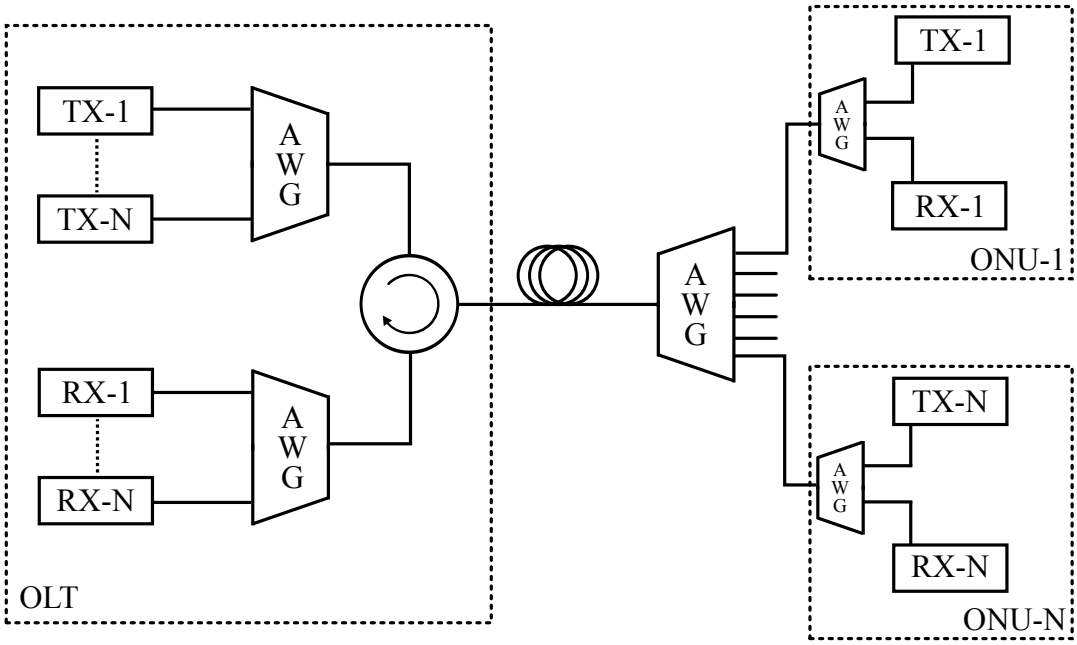

Figure 2.7: WDM-PON general scheme.

in WDM-PON. For the downstream transmission the OLT requires different sources, one for each wavelength (instead of one common laser), the ONU receiver consist of a C/L band tunable filter (for the separation of the upstream and downstream wavelength), and a photodiode.
Regarding the upstream transmission, each ONU is equipped with a Reflective Semiconductor Optical Amplifier (R-SOA) that allows to each subscriber the transmission of upstream information using the optical power sent by the OLT. As depicted in figure 2.8, a continuous optical signal (with fixed wavelength) is sent by the OLT to a ONU. This signal is modulated changing the gain of the semiconductor amplifier, and reflected by the rear mirror. Another configuration for R-SOA is possible using also an EAM (*Electro-Absorption Modulator*) as depicted in figure 2.9. In this case the incoming signal is pre-amplified by the SOA and modulated by the EAM. Finally, the modulated optical signal carrying upstream data is reflected on the rear facet and boosted out by the SOA. This device avoids the presence of a laser at each ONU, since that the optical signal for upstream transmission is provided by the OLT.
Using a R-SOA and a tunable filter for each ONU we get a colorless configuration: each ONU has identical and wavelength-independent components, that allows a considerable costs reduction.

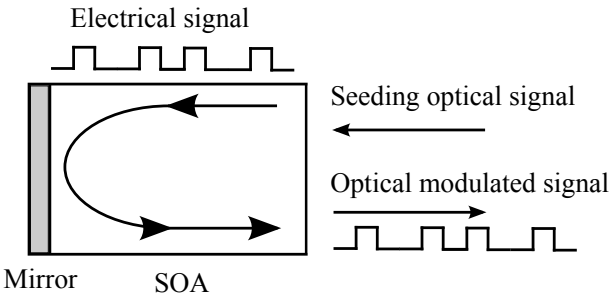

Figure 2.8: Scheme of a R-SOA (Reflective SOA)

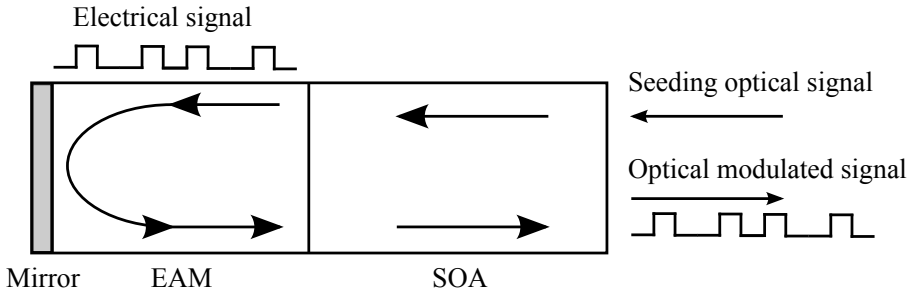

Figure 2.9: Scheme of a REAM-SOA (Reflective Electro-Absorption Modulator SOA)

2.2.3 TWDM PON

In this section TWDM passive optical networks are presented. The architecture is proposed in figure 2.10. Observing figure 2.10, there are four TDM PON stacked together at four different wavelengths: each service providers operates at fixed frequency, handling different ONUs using a time-division protocol. Note that, due to the presence of the power splitter, all the ONUs receive all the optical signals sent by the OLT.
This type of network architecture has different applications. The first one is pay-as-you-grow provisioning: the system could be deployed starting with a single wavelength pair, and it could be upgraded by adding additional wavelength pairs to increase the network capacity. Another possible application is the local-loop unbundling (LLU) using multiple OLT, one for each operator, in such a way that different service providers can share a common infrastructure. The AWG in this case in not part of the OLT, it's used to multiplex different OLTs ports onto a single fiber.
Recently OFDM-based passive optical networks has also been developed, even if from the telelcom operator point of view the TWDM-PON solution is considered as the best solution for residential access networks.

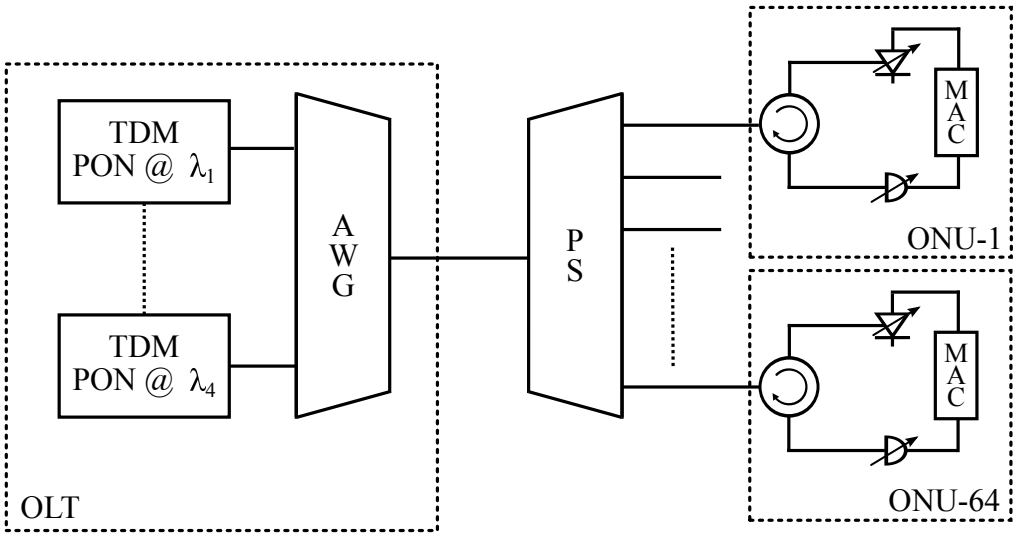

Figure 2.10: TWDM-PON architecture.

2.3 OTDR-based monitoring

In passive optical networks monitoring is an important task for network operator, in order to guarantee the functionality of the network. In conventional optical fiber network the monitoring activity is performed using Optical Time-Domain Reflectometer (OTDR). In this section I briefly present the key concepts of OTDR.
OTDR is the most used instrument for the characterization of optical fibers and optical fibers links. The versatility of this instrument is due to the capacity of measuring local properties of fiber (or fiber link), in other words OTDR gives a complete trend of the fiber local losses.
The fiber parameter which describes the power loss in the fiber is the attenuation constant α. In particular if $P(0)$ is the power launched at the input of a fiber, the transmitted power at distance z from the input is:

$$P(z) = P(0)\exp(-\alpha z) \tag{2.1}$$

The attenuation constant is often expressed in dB/km, from equation 2.1 results:

$$P(z)_{dBm} = 10\log\frac{P(0)}{1mW} - (\alpha 10\log e)z = P(0)_{dBm} - \alpha_{dB}z \tag{2.2a}$$

$$\alpha_{dB} = (10\log e)\alpha \simeq 4.34\alpha \tag{2.2b}$$

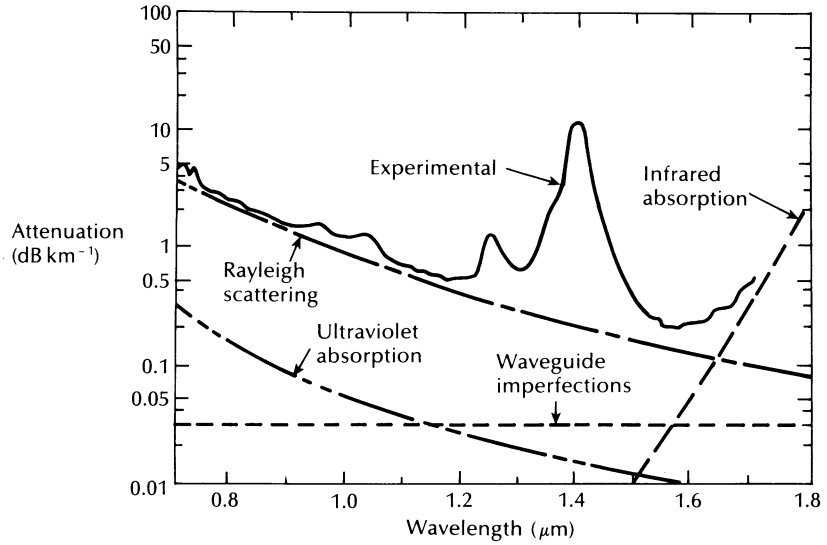

Figure 2.11: Measured attenuation in silica fibers (solid line) and theoretical limits (dashed lines).

As it may be expected, fiber losses depend on the wavelength of light. Figure 2.11 shows the loss spectrum of a silica fiber. Several factors contribute to the loss spectrum with material absorption and Rayleigh scattering being the dominant effects.
The Rayleigh scattering is a fundamental loss mechanism arising from the density fluctuations frozen into the fused silica core during fiber manufacturing, resulting into a non homogeneous refractive index. When the optical radiation crosses these non homogeneous zones, a small fraction of incident light is scattered in all directions.
Rayleigh scattering is the key phenomenon exploited by the OTDR. In figure 2.12 the operating principle of the OTDR is depicted: an optical source produces a pulse which is sent in the fiber through a directional coupler. During pulse propagation, because of Rayleigh scattering, part of the pulse power is backscattered to the fiber input. Finally a directional coupler redirects the backscattered power to a photodiode.
At the generic time t, the photodiode receives the backscattered power of the pulse when it was at the point of spatial coordinate:

$$z = \frac{1}{2}\frac{c}{n}t \tag{2.3}$$

where n is the refractive index of the fiber. The 2 factor at the denominator is due to the fact that the pulse has to cross the fiber two times: at

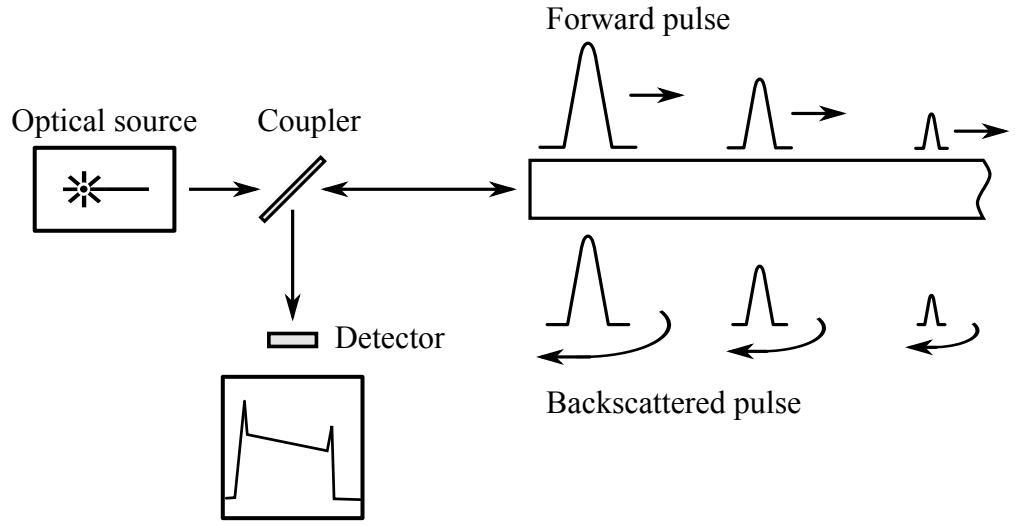

Figure 2.12: OTDR operating principle

first the original pulse goes from fiber input to the the point z, then the backscattered power comes back to the fiber input.

An important parameter in an OTDR-based measures is the pulse duration because it affects the spatial resolution of the measure results. Optical pulses generated by the OTDR have a duration between ten nanoseconds and few microseconds, so each pulse occupies a section of fiber equal to:

$$\Delta = \frac{c}{n}\tau \tag{2.4}$$

Thus the OTDR measure has a spatial resolution related to the pulse duration. In order to understand the relation between resolution and pulse duration is useful to exploit the Minkosky diagram (in figure 2.13).
For the sake of simplicity consider a rectangular pulse. The Minkowski diagram shows the time and space evolution of the pulse: in particular I have highlighted the head and the tail of the optical pulse. From the diagram we can see that the received power at time instant $2t$ is the sum of all the backscattered power in a fiber section of $(c/n)(\tau/2)$. In other words the spatial resolution of the OTDR is equal to half length of the pulse.
In the following table I present the correspondence between pulse width and spatial resolution (considering $c \simeq 3 \cdot 10^8$ and $n \simeq 1,5$).

τ	10 ns	100 ns	1 μs	10 μs
Δ	2 m	20 m	200 m	2 km

Table 2.1: OTDR pulse width and spatial resolution.

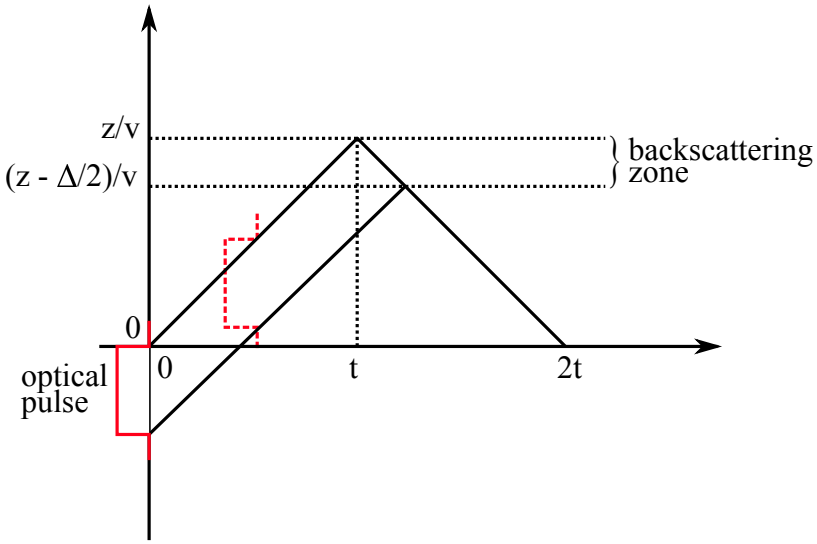

Figure 2.13: Minkowski diagram

The level of backscattered power depends on several factors, in particular considering a fiber section of Δz (with Δz small enough to enable losses negligence) we get:

$$P_d = (S_d S_c)\Delta z P_i = S \Delta z P_i \tag{2.5}$$

where S_d represents the portion of power that is scattered because of the Rayleigh effect ($S_d \sim 1/\lambda^4$), and S_c is the portion of the scattered power that is recaptured by the fiber and driven to the beginning of the fiber. P_i is the peak power of the pulse in the fiber section where the backscattering takes place.

In order to compensate to the extremy low level of the backscattered power received from the OTDR an avalanche photo-diode (APD) is used. Furthermore an high number of measurements must be made on the same fiber (or fiber link), exploiting the fact that the signal-to-noise ratio (SNR) increases with the square root of the number of measurements.

Chapter 3

Experimental setup

The purpose of the thesis is the experimental implementation and evaluation of a monitoring system for passive optical networks. In previous chapter I have introduced passive optical networks, I now present the experimental setup describing the monitoring scheme, adopted devices and observed problems. The idea is to realize a multi-wavelength OTDR: referring to the proposed PON schemes (see figures 2.6, 2.7 and 2.10) the task was to implement a scheme that is able to perform monitoring activity in all the configurations proposed.

3.1 Monitoring scheme

The monitoring scheme is proposed in figure 3.1. In order to get the possibility of tuning the wavelength an external tunable laser is used, which continuously emits optical power at the selected wavelength. So as to obtain the same pulses of the OTDR I used an Acusto-Optic Modulator (AOM) which is controlled by a Pulse Generator (PG). The generation of the pulse works as follow:

1. the OTDR generates one (or more) pulse;
2. this pulse is transformed in an electrical signal by a photodiode, and it is sent to the pulse generator as a trigger signal;
3. when the pulse generator receives the electrical signal, it generates a rectangular pulse (of specified duration) that open the AOM.

Once the pulse exits from the modulator, it passes through the circulator and it is sent to the fiber under test using an AWG or a power splitter. Thus, the backscattered power is sent to the OTDR, by the circulators.

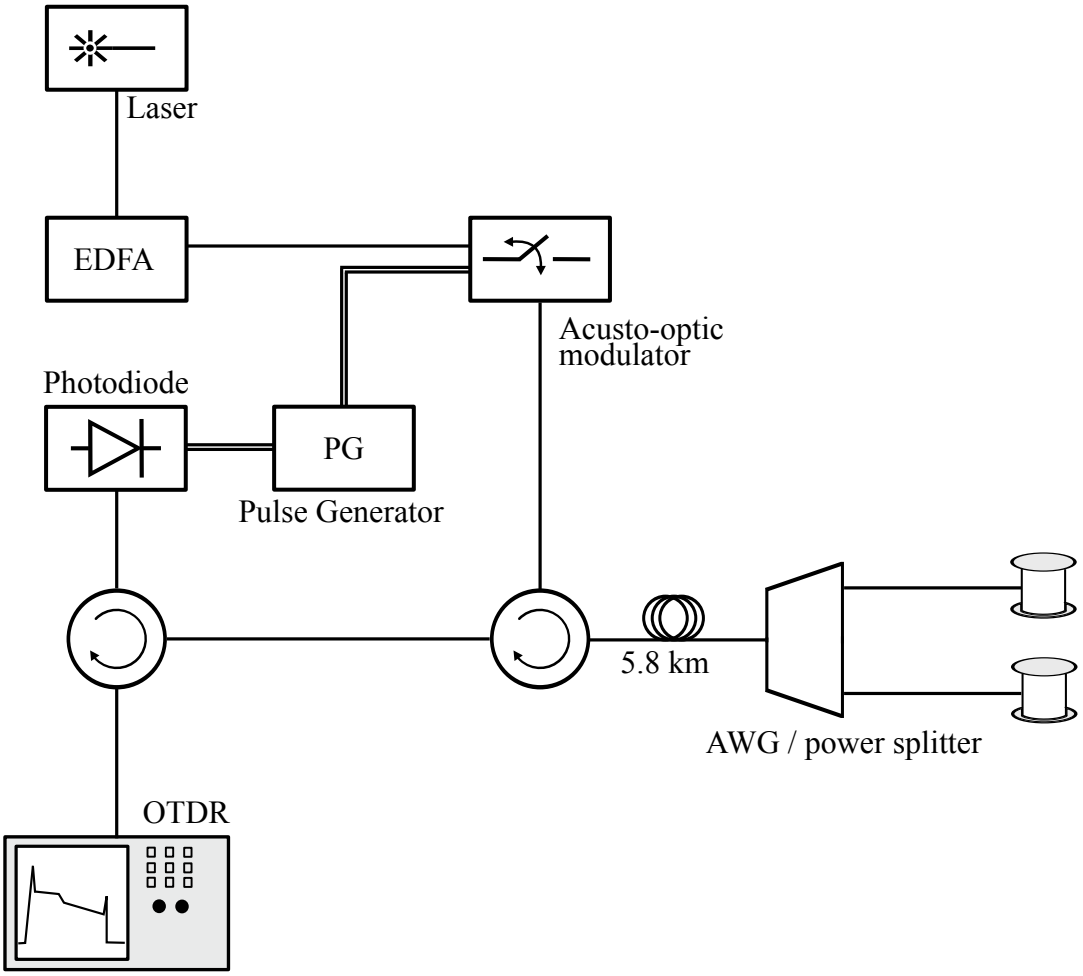

Figure 3.1: Monitoring scheme

3.2 System characterization

In this section I present some preliminary measures performed to characterize the system. In particular I have investigated the pulse characteristics as the pulse shape, the pulse duration, and power peaks of the pulse with respect to a conventional OTDR.

3.2.1 Pulse shape

First of all I need a reference measure for a typical OTDR pulse. I have performed this test using the simple setup in figure 3.2. The OTDR pulse is converted into an electrical signal and shown on the oscilloscope. The photodiode has a conversion ratio of 45 mV/mW, I have use an attenuator (-19.07 dB) in order to prevent the photodiode saturation. I have executed the measure using two different pulse duration, the signals shown on the oscilloscope are showed in figure 3.3 and 3.4.
From the oscilloscope we get that the average voltage of the pulse is about 30mV, taking into account the conversion ratio and the attenuator, the OTDR output power is:

$$P_{OTDR-OUT} = 17.33dBm \tag{3.1}$$

Observing figure 3.3 and 3.4 I can note that both the pulses have a rise time of about 10 ns.
I can now compare these pulses with the ones obtained from two configurations:

- first I observe the signal exiting from the system using only the acusto-optic modulator: this measure allows us to evaluate the rise time of the AOM and the pulse duration with respect to the setted one;
- second I repeat the same measure including the EDFA in order to take into account also the effect of the amplifier.

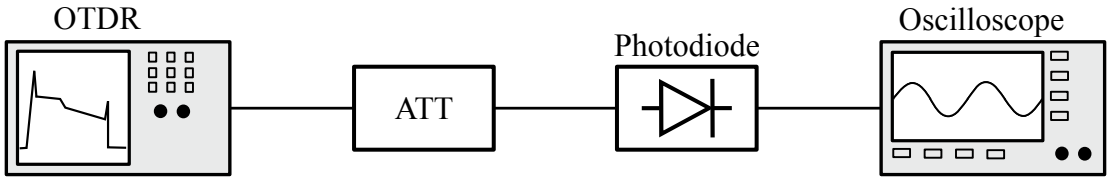

Figure 3.2: OTDR pulse measure setup.

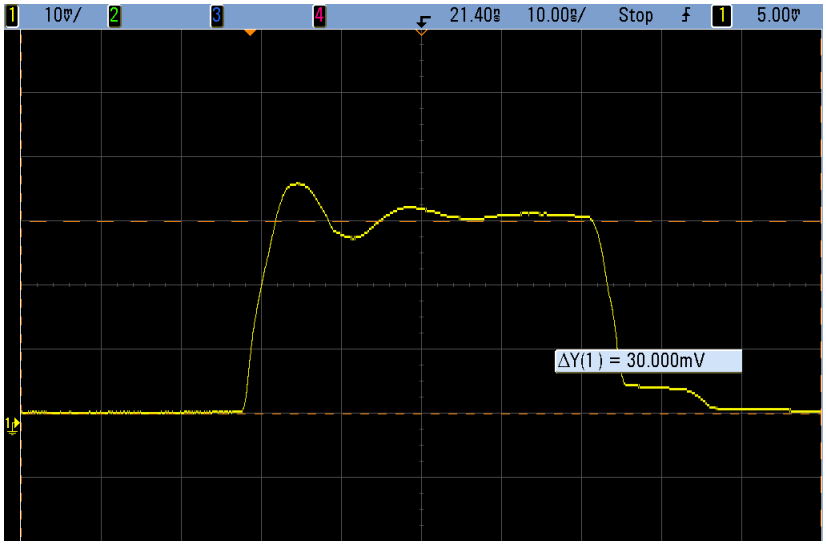

Figure 3.3: OTDR pulse (50 ns).

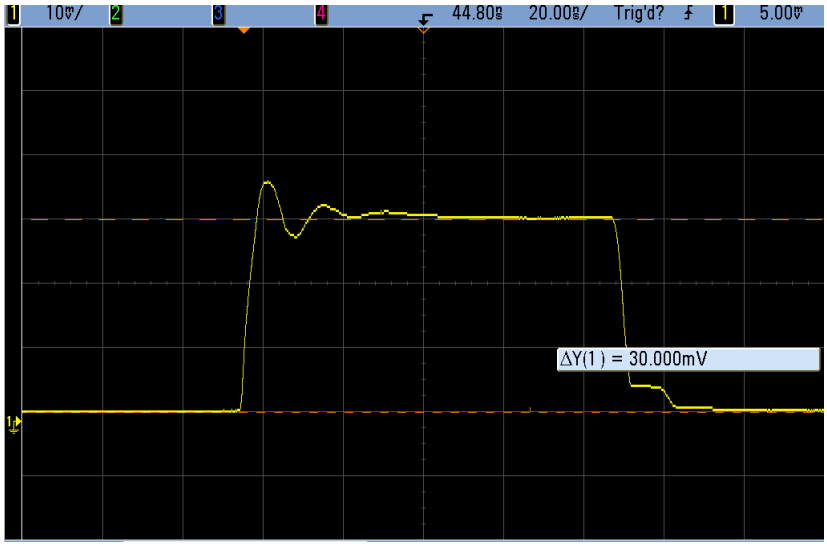

Figure 3.4: OTDR pulse (100 ns).

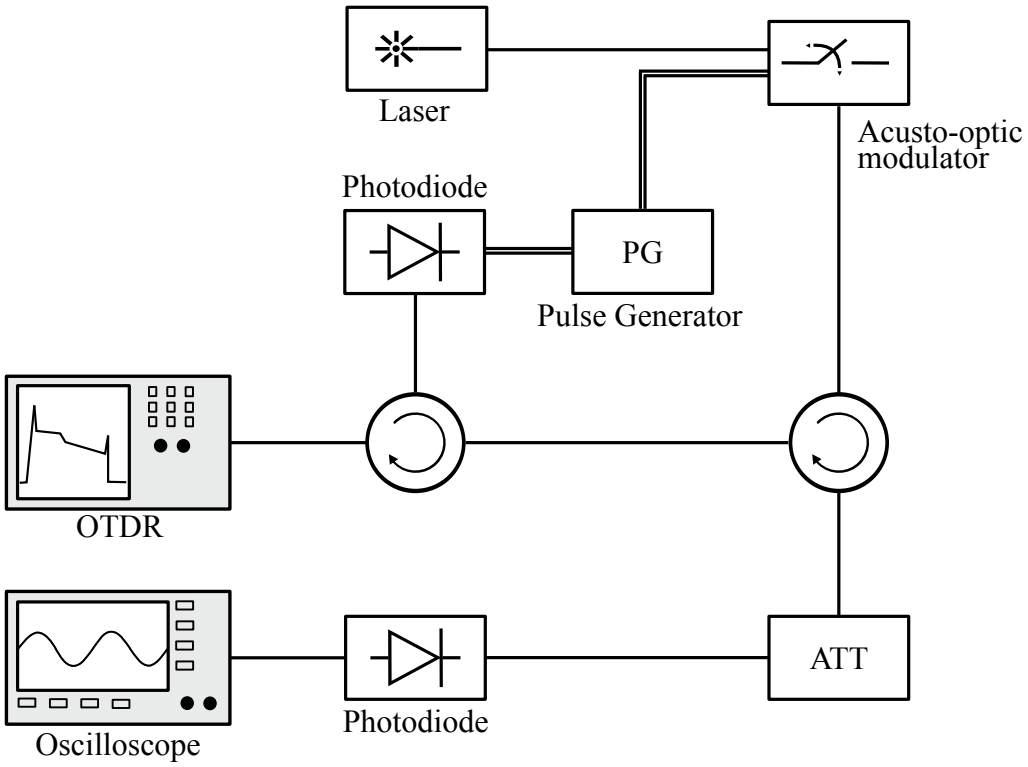

Figure 3.5: Setup for evaluating AOM performances.

To the aim of evaluating the AOM performances, I adopt the scheme in figure 3.5. Observing figure 3.6a we can note that the pulse is not rectangular. The reason of this phenomenon can be understood looking at the other figures (from 3.6b to 3.6d): in these cases we can observe that the pulses are actually rectangular and the acusto-optic modulator has a relatively long rise time of about 60 ns, then if I set the pulse duration to 50 ns the AOM can not open itself completely. Again, it can be also noted that in the last three cases, with pulse duration longer than 50 ns, the signal peak is about 4.4 mV and it does not change with a different pulse width. Regarding the power level, the laser is set to 0 dBm, taking into account the presence of the attenuator (5 dB in this case), and using the same photodiode as the previous case (45 mV/mW), we get:

$$P_{OUT-AOM} = -5.1dBm \tag{3.2}$$

From a set of measures in continuous-time regime (with the AOM open) I have verified that the modulator introduces an insertion-loss of about 5 dB.

Finally I have to consider the pulse with the presence of the EDFA for

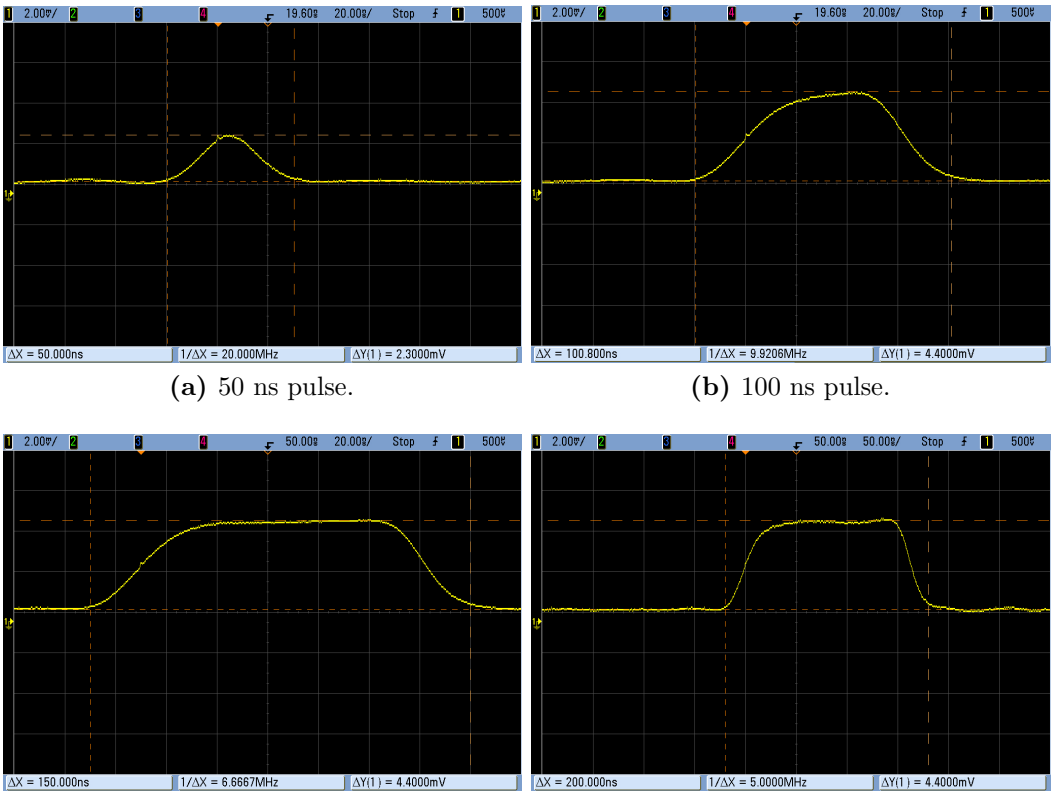

(a) 50 ns pulse. **(b)** 100 ns pulse.

(c) 150 ns pulse. **(d)** 200 ns pulse.

Figure 3.6: Total pulse exiting from the AOM.

different gains. The adopted scheme is very similar to the previous with the exit of the laser connected to the erbium amplifier, as depicted in figure 3.7. The laser power level was 0 dBm and an attenuator provided 19.15 dB. In this case I have fixed the pulse duration (in the pulse generator) to 100 ns and I have observed the total pulse exiting from the modulator for different gains of the EDFA, in particular with pump current of 350 mA, 400 mA, 450mA and 500mA. The resulting pulses are shown in figure 3.8. Except for the case with pump current at 350 mA (figure 3.8a), where the intensity of the pump is not high enough, I can observe that the pulse shape is not heavily modified modified with respect to the case in absence of the EDFA. In particular comparing figures 3.6b with 3.8c, the pulses are quite similar.

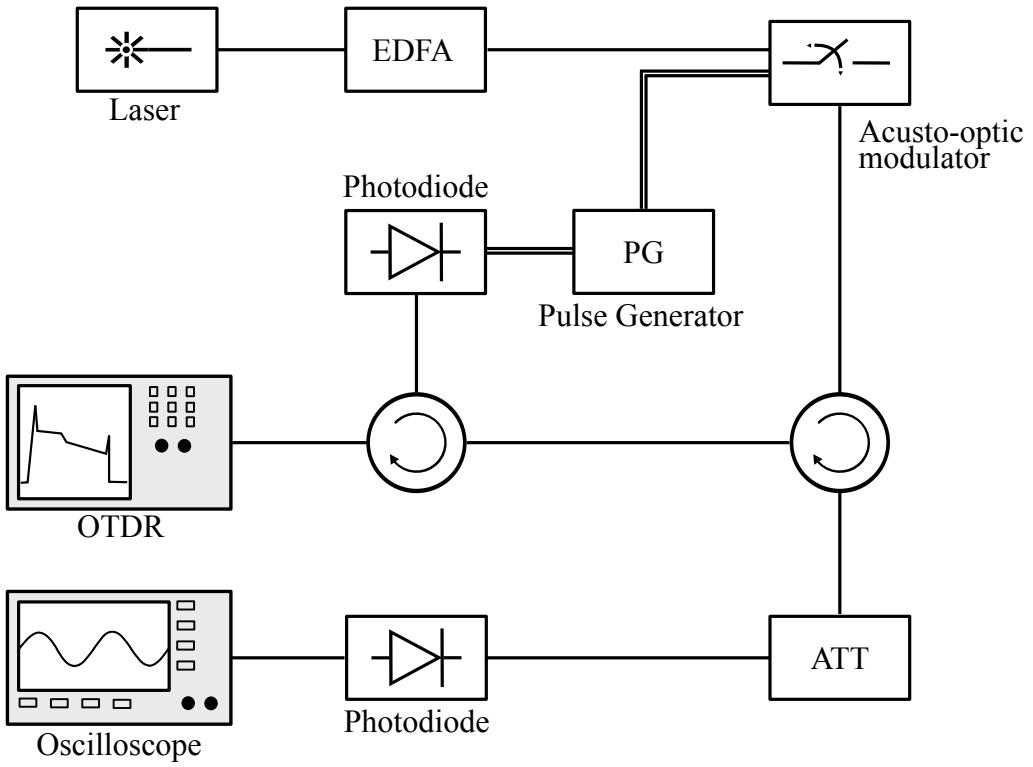

Figure 3.7: Setup for evaluating EDFA influence.

I_p (mA)	V_{peak} (mV)	$P_{OUT-AOM}$ (dBm)
350	2	5.63
400	2.88	7.21
450	4.15	8.81
500	5.45	9.97

Table 3.1: Power level measured at the photodiode for different pump current.

Regarding the power level, I summarize the results in table 3.1: recalling that for this set of measures the laser output power is set to 0 dBm, I have reached with relatively low pump current an high level of power at the output of the AOM, even if it is not comparable with the level measured using the OTDR (see figures 3.3 and 3.4).
For next measure I have made use of a Pirelli© laser with higher output levels in order to reach an exiting power comparable with respect to a typical OTDR.

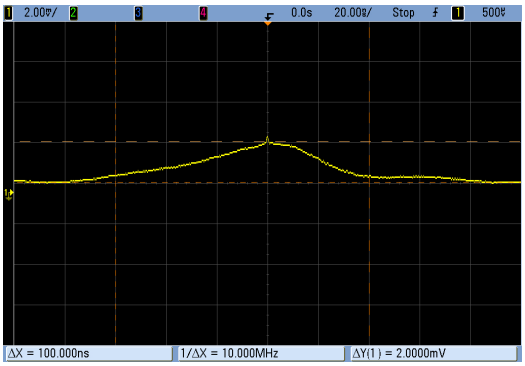

(a) 350 mA and 100 ns pulse.

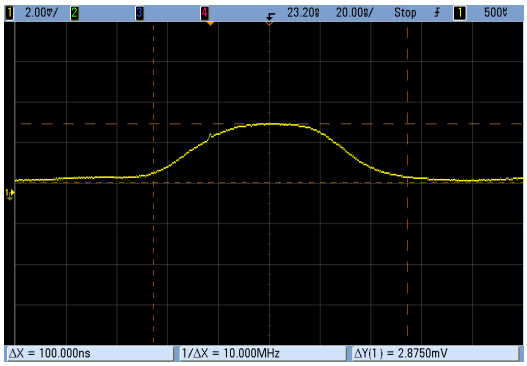

(b) 400 mA and 100 ns pulse.

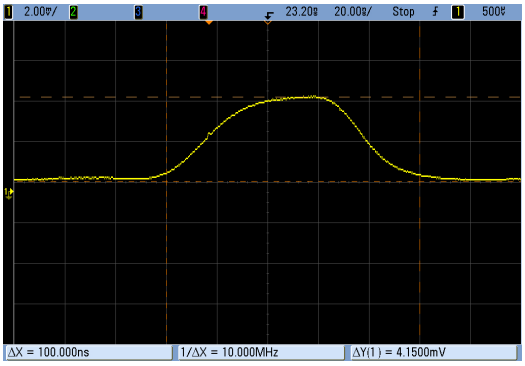

(c) 450 mA and 100 ns pulse.

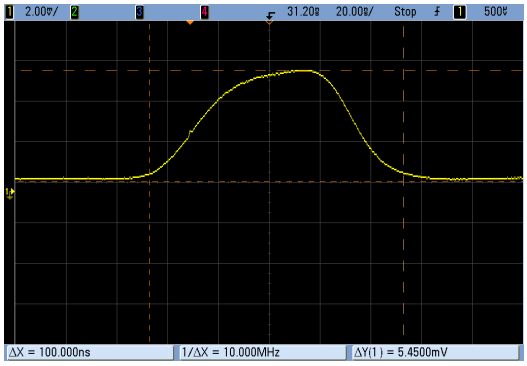

(d) 500 mA and 100 ns pulse.

Figure 3.8: Total pulse exiting from the AOM with EDFA.

3.2.2 Pulse spectrum

As said before the task was to test the monitoring scheme using both an AWG or a power splitter. In the first case an important measure to be performed is the verification of the spectra at the input of the AWG. In particular I have used an AWG with four exiting channels at 1533 nm, 1541 nm, 1549 nm and 1557 nm.
The main aspect that was to be evaluated is the contribution of the amplified spontaneous emission (ASE) of the EDFA. In this case the setup is quite simple as well and is shown in figure 3.9. I have performed this measure with the acusto-optic modulator open, setting different pump current for the EDFA. In the following figures we can see the resulting spectra with the laser set to 1533 nm.
Figures 3.10, 3.11 and 3.12 clearly show the presence of the ASE. In particular, as expected, by increasing the pump current of the EDFA also the ASE power has a small increment.

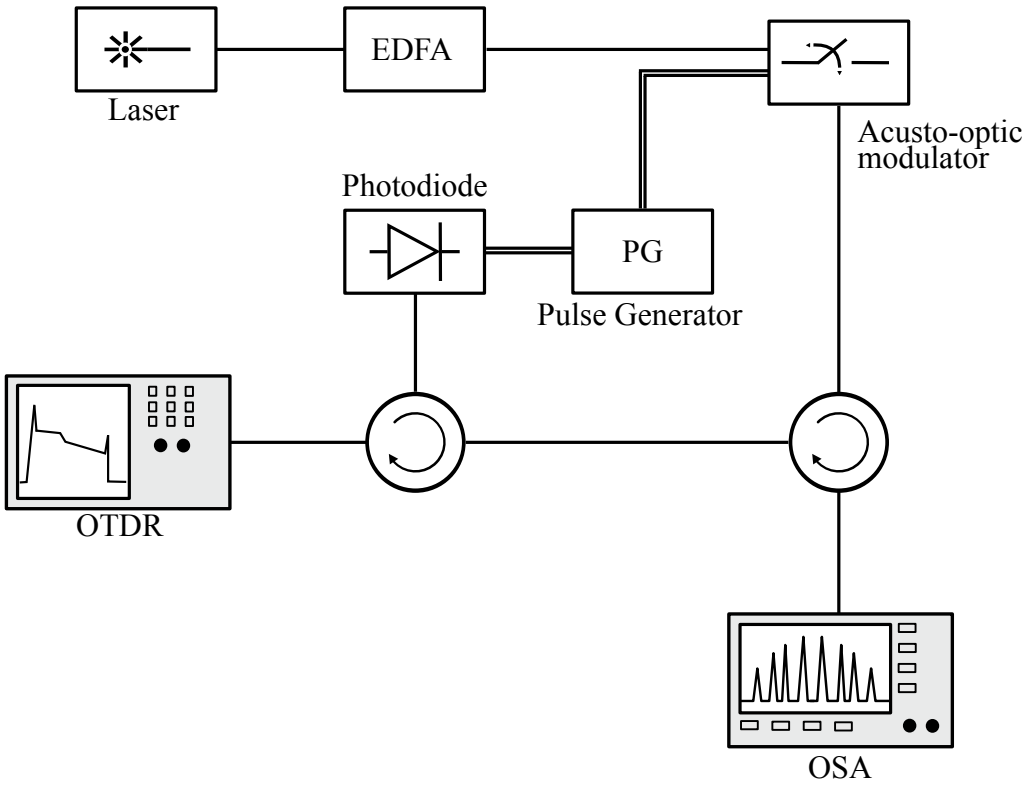

Figure 3.9: Setup for AWG input spectra evaluation.

Even though the laser signal is narrow band, at the AWG input I get a signal with larger bandwidth due to the spontaneous emission of the EDFA, so a non-negligible amount of optical power is sent in other AWG branch and this phenomenon could affect the measurement.

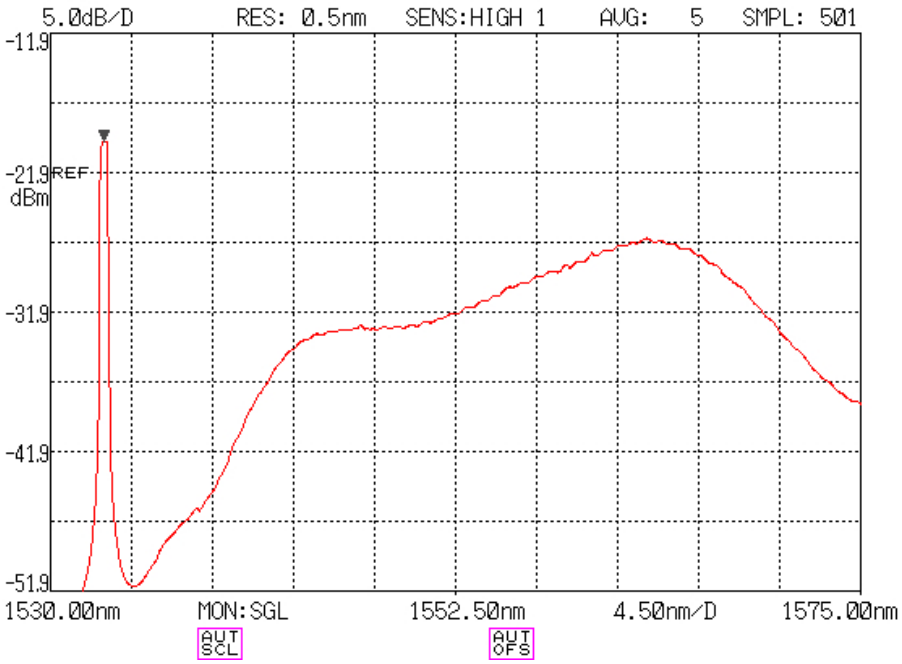

Figure 3.10: Input spectra at the AWG with EDFA pump current at 310 mA

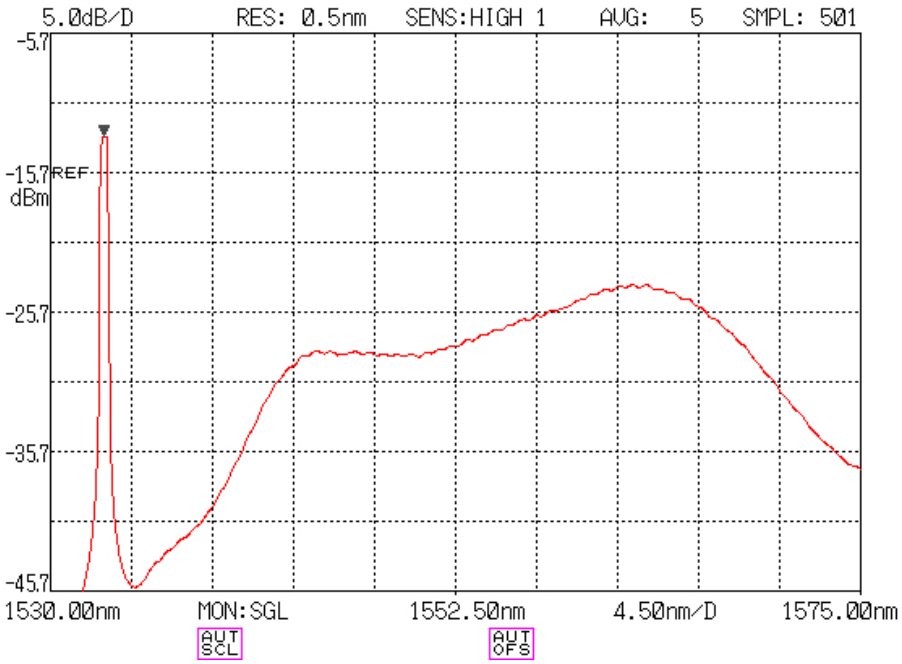

Figure 3.11: Input spectra at the AWG with EDFA pump current at 320 mA

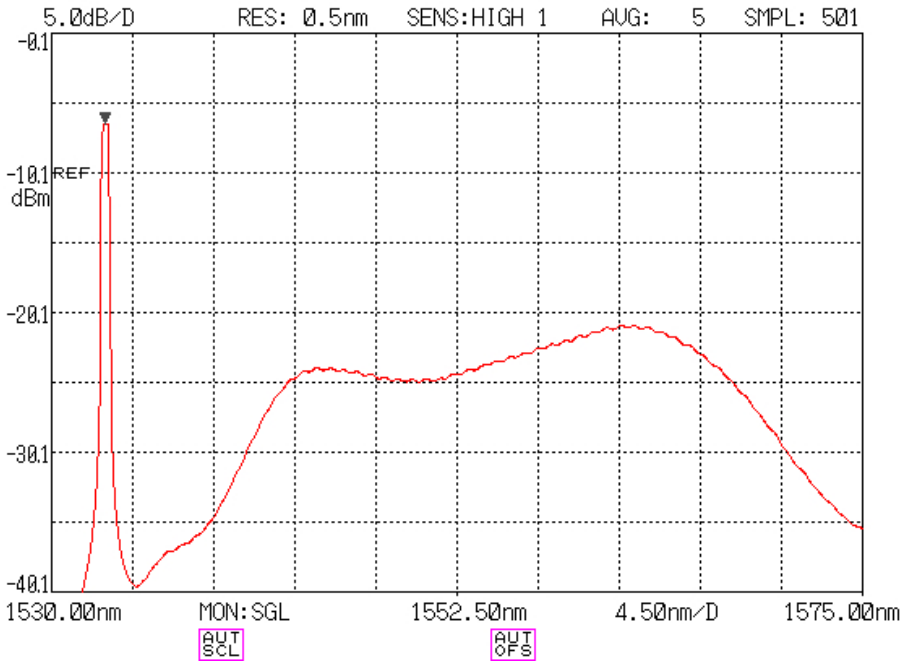

Figure 3.12: Input spectra at the AWG with EDFA pump current at 340 mA

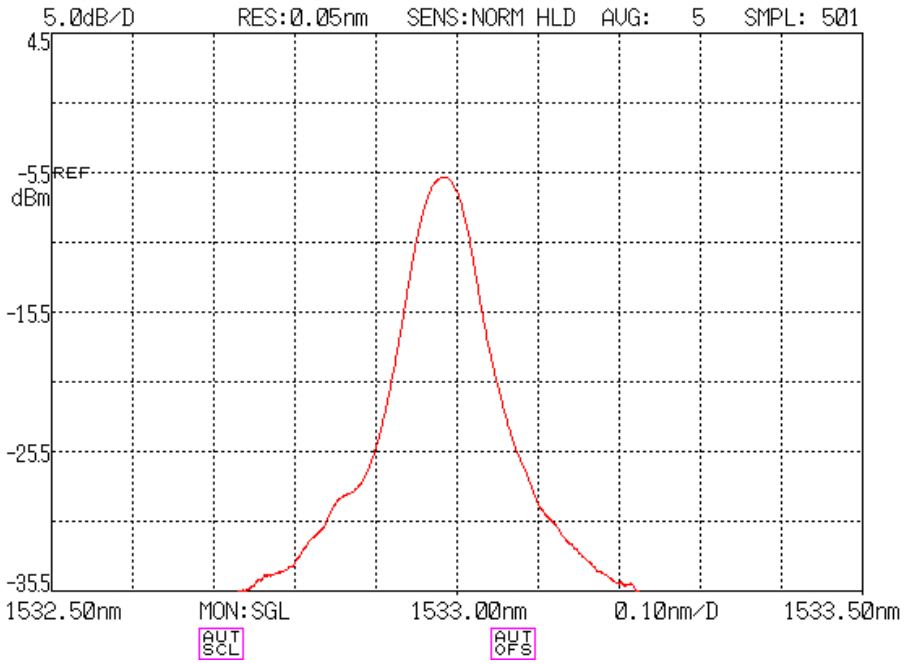

Figure 3.13: Peak at 1533 nm with EDFA pump current at 340 mA

Chapter 4

Results

In this chapter I present the measures resulting from several test setup; in particular I have used both an AWG and a power splitter at the remote node, and a reduced number of branches with respect to a real network configuration. Furthermore the length of the fiber connected to the remote node is higher with respect to a real passive optical network (in general the length of the link between the remote node and the ONU is up to 5 km). These results allow us to understand the behavior and the limits of the system. I arranged six different test setup with different branch numbers and terminators at the end of the fibers. As shown in figure 3.1 for all these tests I have used a launch cable of 5.8 km as in a typical PON setup.
With regard to the system settings I have adopted (unless otherwise specified):

- pulse width of 150 ns (at the pulse generator);
- output laser power $P_{LASER} = 10dBm$;
- EDFA pump current $I_P = 570mA$.

4.1 Configuration 1

In this simple configuration I used four fiber connected to the AWG. At the end of the fibers that were not under test, I inserted an absorbing terminator in order to avoid reflections. The resulting traces are shown in figure 4.2.

I can note that at the beginning of every trace there is an high peak which is due to the reflection of the launch fiber connector. The presence of this peak causes a wrong trace analysis by the OTDR because the instrument interprets this peaks as the fiber-end peak. Furthermore the traces obtained

from this scheme are more noisy with respect to a typical OTDR trace. This is due to the presence of ASE (of the EDFA): because of the amplified spontaneous emission, a small amount of power is sent also in the branch that are not under test. Note that this phenomenon causes the presence of fiber end peaks of other branches: observing figure 4.2a we notice the peaks at 20 km (related to the 1541nm branch) and at 15 km (related to the 1549 nm branch).
Looking at the traces, I can see that the peak at 5.8 km appears in all the traces: it is due both to the connector of the launch fiber and the AWG connector, because they are very close it's not possible to distinguish their peaks in the OTDR trace. Finally I can note that all the four traces show correctly the end fiber peaks even if in all the traces there are some spurious peaks beyond the fiber end.

4.2 Configuration 2

Let us check now the capability of the identification of a fiber break. To this aim I have exploited the following configuration: I have used three channels of the AWG, in particular in the 1557 nm branch I have connected two different reels. As in previous tests I have used non-reflective terminators.

In order to simulate a fiber break I opened the connector between the reels and we observed the outcoming trace. In figure 4.4 I report both the trace obtained without any modification (in red) and the trace obtained opening the connector in the 1557 nm branch (in blue), I can note that:

- in the 1541 nm trace there are no differences between the red and the blue one;
- in the 1549 nm trace, the blue trace presents a new peak at about 16

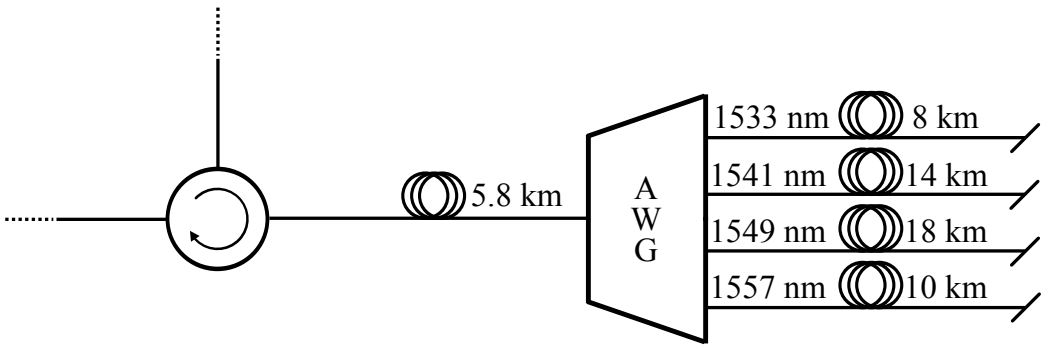

Figure 4.1: Configuration 1

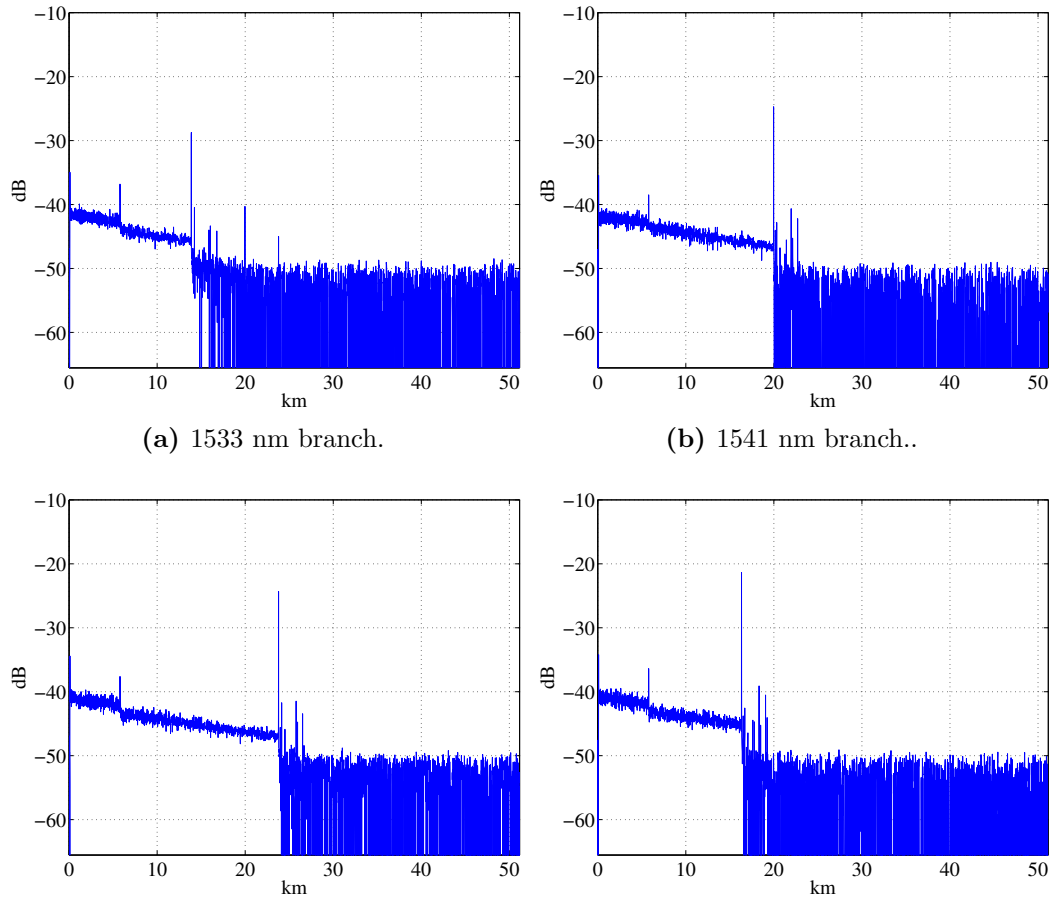

(a) 1533 nm branch. **(b)** 1541 nm branch..

(c) 1549 nm branch. **(d)** 1557 nm branch.

Figure 4.2: Configuration 1 traces.

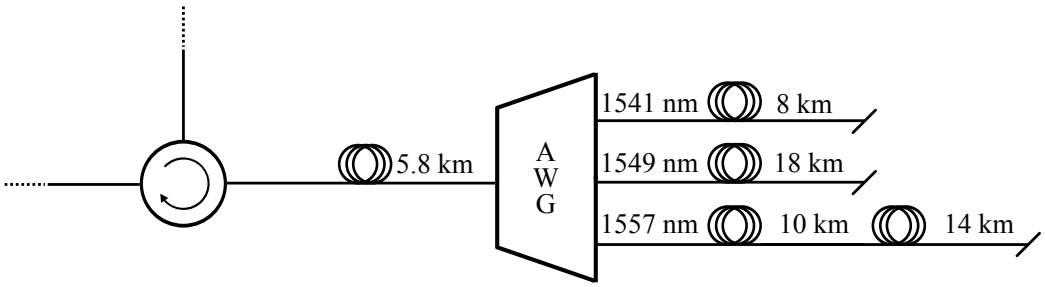

Figure 4.3: Configuration 2

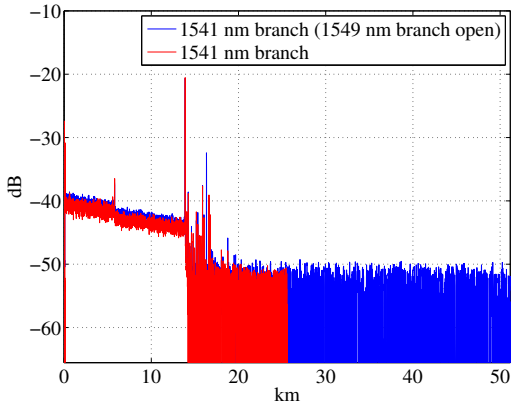

(a) 1541 nm branch.

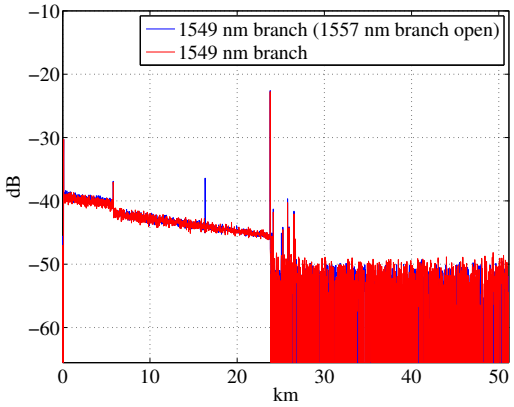

(b) 1549 nm branch.

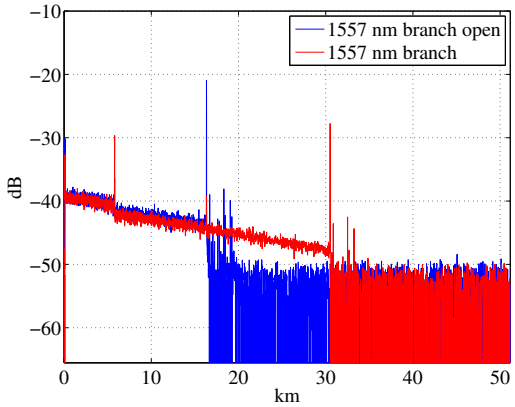

(c) 1557 nm branch.

Figure 4.4: Configuration 2 traces.

km due to the reflection at the open connector (the previous trace at 1541 nm does not present a peak because the fiber is too short), no other changes are evident;

- in the 1557 nm trace we can see an important change between the red and the blue trace; opening the middle connector, the fiber-end peaks move to about 16 km.

Thus in this case I can identify the break observing the trace modification of the corresponding branch. Other traces (only one in this experiment) show only the appearance of a new peak with respect to the original configuration.

4.3 Configuration 3

As mentioned in section 2.2, in WDM-PON and TWDM-PON the ONUs are equipped with a filter and a R-SOA, thus I am interested in testing the system using frequency-selective branch terminations. In this section I present a 2-branch configuration without any type of termination, the connector at the end of the fiber are simply open (figure 4.5). In the next paragraph I introduce frequency-selective terminations in such a way that we can compare the results.

In figure 4.6 I have reported the resulting traces. The main differences from previous measures consist in the presence of the final peaks of the fibers: in figure 4.6b both fiber-end peak are clearly visible. On the contrary, the reflection due to the middle connectors is not visible. Regarding the measures obtained from a break simulation, the behavior is similar to the previous case: the branch interested by the break changes the final peak position and the other branch shows a new peak. The presence of multiple peak in the trace without configuration alterations (see figure 4.6b) could not seem a problem because, knowing the network configuration, the peaks position has a precise meaning. Thinking to an automatic system the presence of multiple peaks can make trace analysis more difficult, specially if the fibers have similar length. In the next configuration I introduce the frequency-selective terminations both to be closer to a real network configuration and to avoid the presence of multiple peaks.

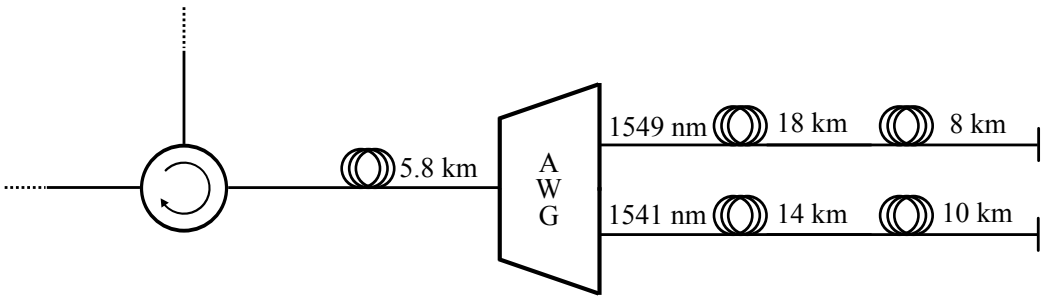

Figure 4.5: Configuration 3

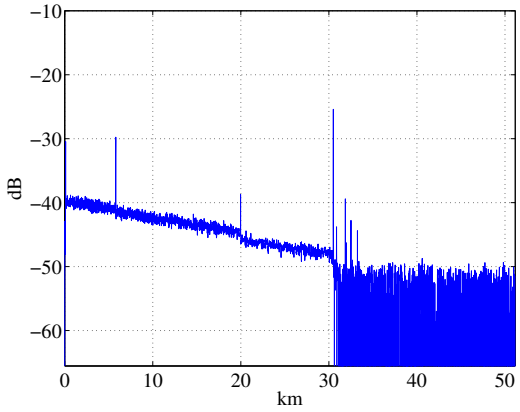

(a) 1541 nm branch.

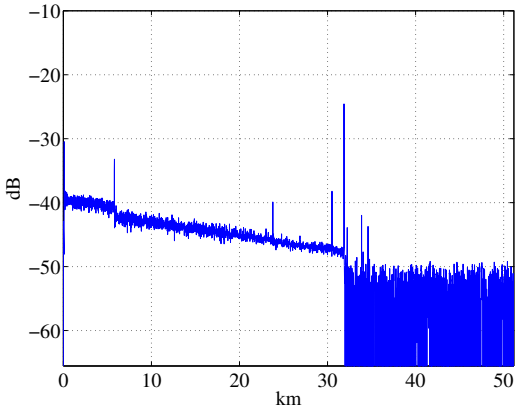

(b) 1549 nm branch.

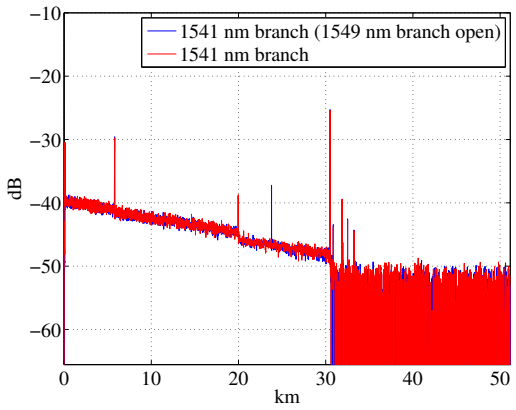

(c) 1541 nm branch (1549 nm branch open).

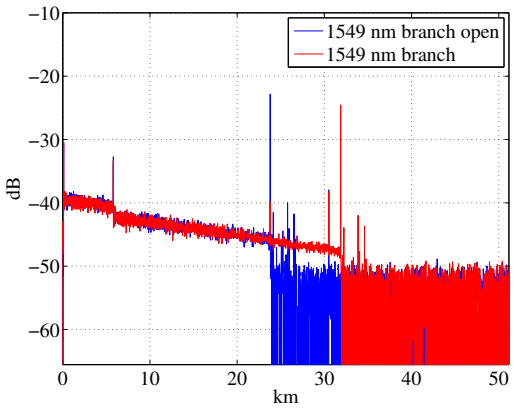

(d) 1549 nm branch (1549 nm branch open).

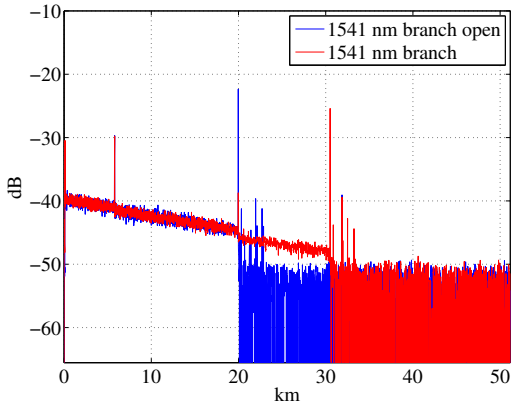

(e) 1541 nm branch (1541 nm branch open).

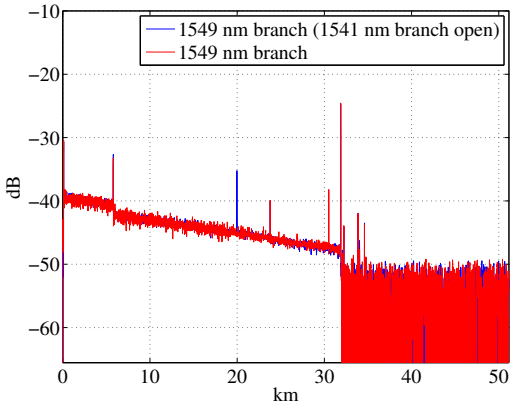

(f) 1549 nm branch (1541 nm branch open).

Figure 4.6: Configuration 3 traces.

4.4 Configuration 4

In this configuration frequency-selective terminations are used, in particular I have adopted a tunable FBG (Fiber Bragg Grating) and a tunable pass-band filter followed by a wide-band mirror. In figures 4.8 and 4.9 I present the characterization of the pass-band filter and fiber Bragg grating respectively, using a white-light source. Once the laser is set at the correct wavelength the tuning process for the PBF is performed in two steps: first, using a power meter I tuned the device maximizing the received power, then I use a white-light source to check the precision of the tuning and correct it if necessary. The tuning process for the FBG differs because in the first step I want to minimize the power at the output port (the wavelength of interest is reflected to the input port).
The action of this devices can be seen accurately comparing figures 4.6b and 4.10b: in the second case the presence of the filter avoids the appearance of the smaller peak in correspondence with the end connector of the 1541 nm branch.
In this case I have also simulated a fiber break in both the branch, but the results are very similar with previous cases (figures 4.10c and 4.10d). Until this point I have considered just failures that causes an high reflection, using this configuration I have considered also a non reflective malfunction like a fiber bend. In order to simulate this event I have connected to the middle connector a non reflective terminator. In figures 4.10e 4.10f I can see the corresponding traces. I can notice that this situation generates a trace similar to fiber break but with a reduction of peak intensity, however a failure identification is possible.

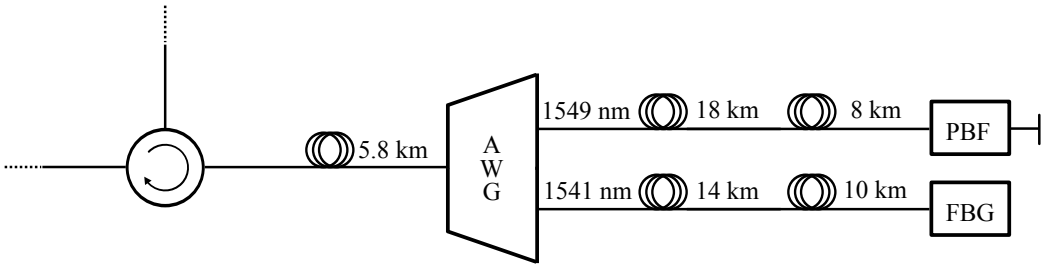

Figure 4.7: Configuration 4

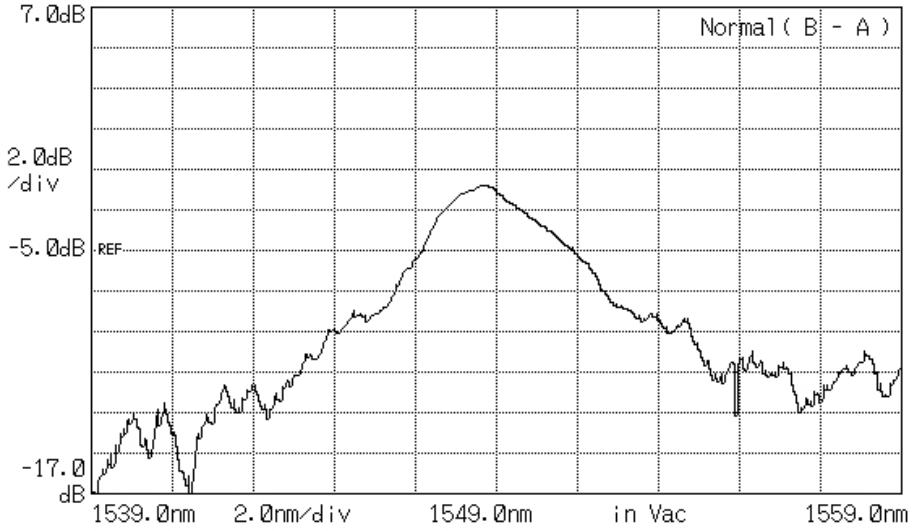

Figure 4.8: PBF tuned at 1541nm

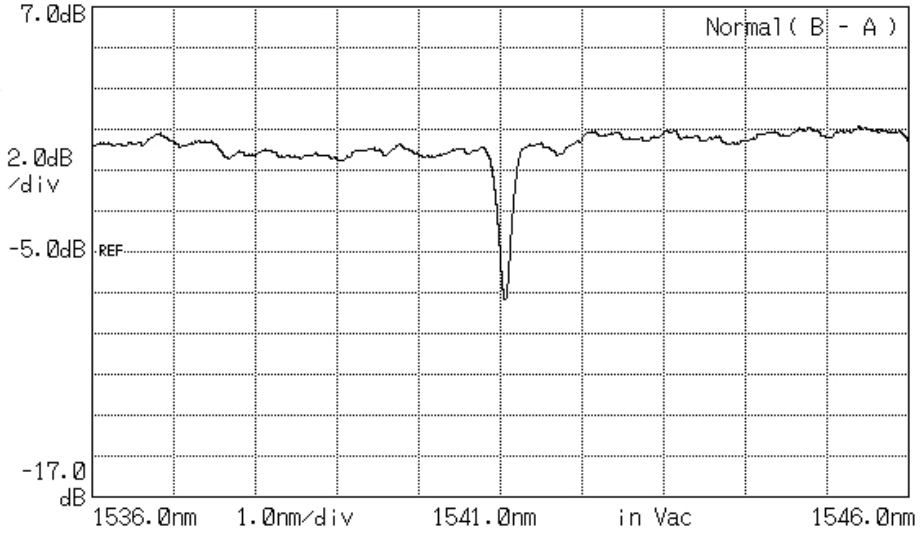

Figure 4.9: FBG tuned at 1549nm

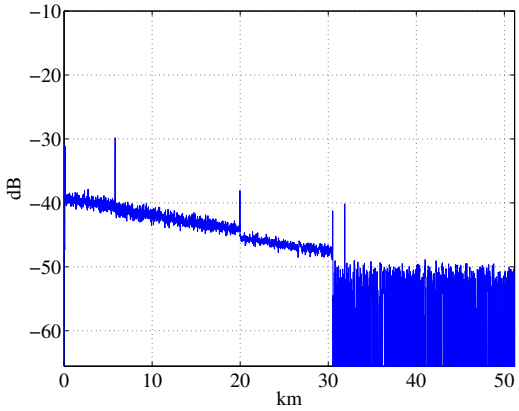

(a) 1541 nm branch.

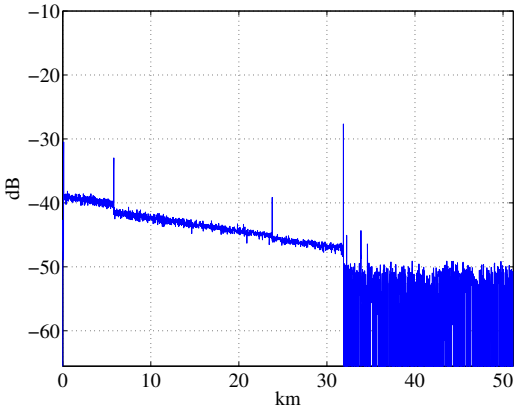

(b) 1549 nm branch.

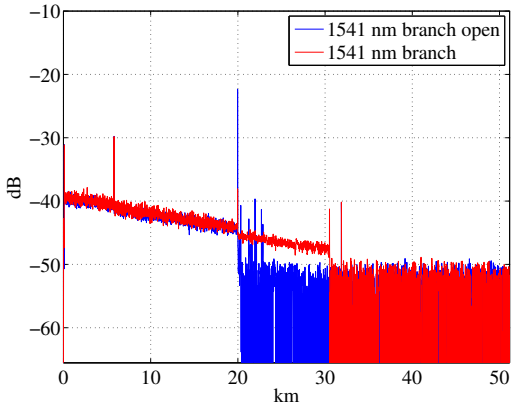

(c) 1541 nm branch (1541 nm branch open).

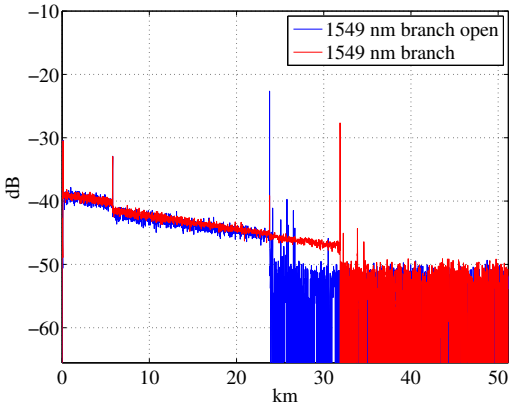

(d) 1549 nm branch (1549 nm branch open).

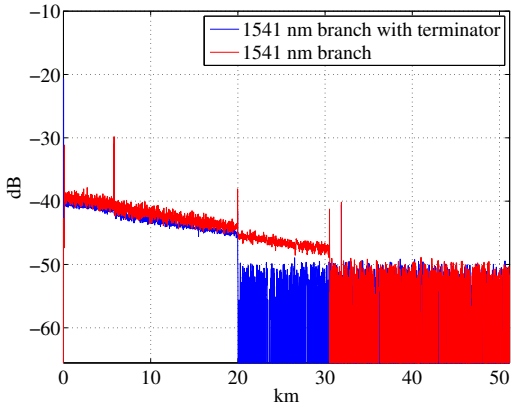

(e) 1541 nm branch (1541 nm branch terminated).

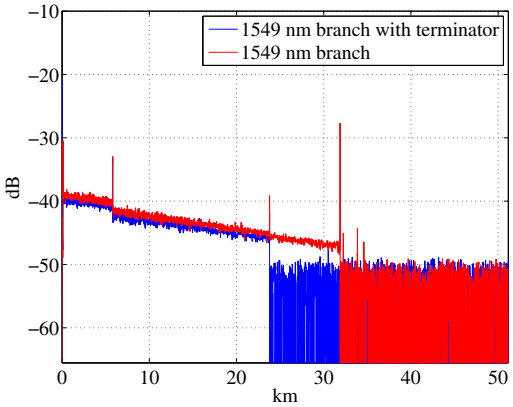

(f) 1549 nm branch (1541 nm branch terminated).

Figure 4.10: Configuration 4 traces.

4.5 Configuration 5

Finally I have to test the behavior of the monitoring scheme using a power splitter as remote node. The configuration is shown in figure 4.11. In this case I have used a 50/50 power splitter maintaining the same branches as before. The only difference with respect to the previous test is the set of the wavelength associated with the branches: using the power splitter I have not used the wavelengths of the AWG so I have chosen 1540 nm and 1555 nm because increasing the spectral distance I have tried to increase the pass-band filter and the FBG performances.
In figure 4.12 I present the resulting traces. I can note some important difference in comparison with configuration 4. First, the measures in normal condition are more noisy than the previous, in figures 4.12a and 4.12b I can note that there are some spurious peaks beyond the final peaks. Furthermore I can note the presence of the middle and final connectors peaks in both traces. This is due to the fact that the power splitter simply divides the amount of optical power between the two branches, thus a higher power is sent into the channel that is not under test with a resulting increased reflection. The frequency-selective termination can not remove these peaks because during propagation, the pulse encounters the middle connector, the connector between the fiber and the termination, and the the final connector (or the mirror in the case of the 1555 nm branch), thus the reflection at the middle connector occurs before the "filtering" termination. This phenomenon, as I have explained in configuration 3, could be a problem in the case of an higher number of branches (specially in case of similar lengths).
With regard to the break detection, observing figures 4.12c and 4.12d, I can notice that, unlike the AWG case, the opening of the middle connector does not cause an evident trace changing, and this is due to the amount of power split in every branch.

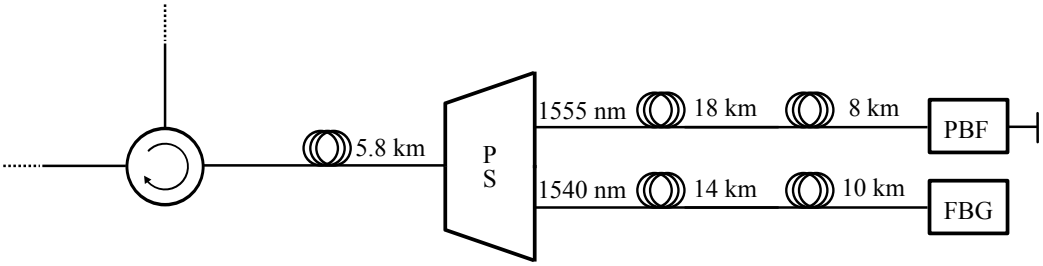

Figure 4.11: Configuration 5

It is still possible to identify the failure (or in any case a trace alteration) observing the position and the intensity of the peaks: the final peak disappears, the middle peak increases the intensity and some spurious peaks appear. The simulation of a non-reflective failure has a sort of dual behavior, the traces in figures 4.12e and 4.12f result from the insertion of non-reflective termination in the middle connector. In this case as well there are not clear trace modifications but it is still possible to find out the anomaly: as in the previous case the final peak disappears and in the correspondence of the damage the peak reduces its intensity and a loss step appears (similar to a splice loss).
Thus if a power splitter is used it is still possible to identify failures even if an high number of branches could make the trace analysis quite difficult.

4.6 Configuration 6 with a modified scheme

In order to try to get better performances using a power splitter I have modified the original scheme (figure 3.1) adding a tunable pass-band filter (PBF) between the circulators: in this way the backscattered power is filtered before the OTDR input. The modified scheme is proposed in figure 4.13. The system works exactly as the original one with the only difference that the center wavelength of the pass-band filter must always correspond with the laser wavelength. Note that if the channels are very narrow, the pass-band filter must have very high performance.
The test configuration for this scheme is shown in figure 4.11. In this case I have used two FBG as frequency-selective termination tuned at 1549 nm and 1555 nm; this choice guarantees the best wavelength spacing for these two particular FBG. The resulting traces are presented in figure 4.15.
Observing figure 4.15b I can note that the final peaks of both the branches are still present even if there is a low reduction of intensity in the peak at 31 km. Regarding the break simulation (figures 4.15c and 4.15d) the best results are obtained measuring the 1555 nm branch (possibly because the tuning was more precise): I can note that the presence of the filter makes the trace modification more evident with respect to the previous tests. Finally, looking at the traces obtained with non reflective termination (figure 4.15f) I can see that the filter achieves a better results: even if more noisy, the trace is quite similar to the one obtained with the AWG configuration (see figure 4.10e and 4.10f). Let us underline that the evaluated performance depend on the adopted filter and on the tuning process, a filter with better performance could reach best results.

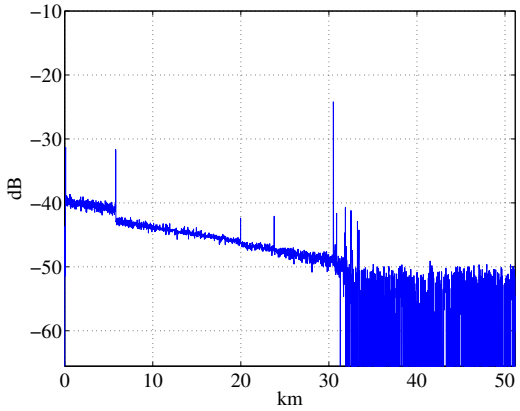

(a) 1540 nm branch.

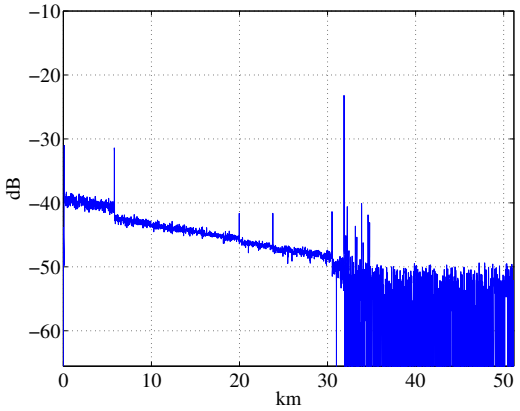

(b) 1555 nm branch.

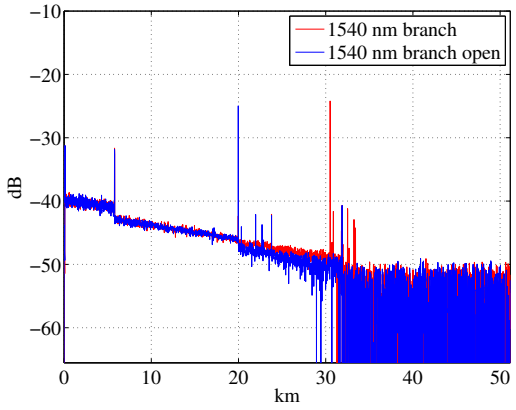

(c) 1540 nm branch (1540 nm branch open).

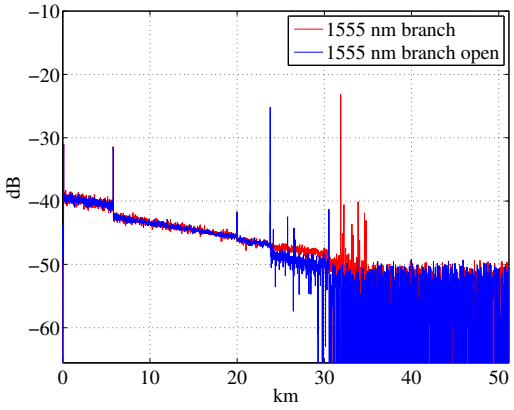

(d) 1555 nm branch (1555 nm branch open).

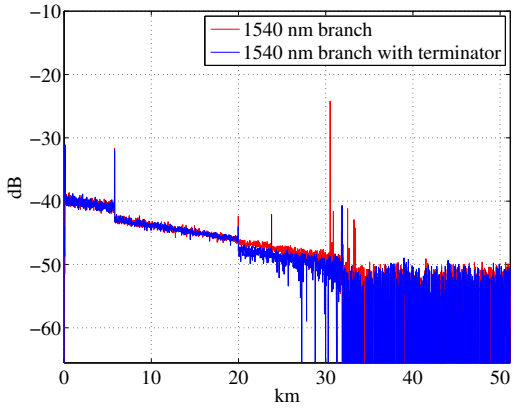

(e) 1540 nm branch (1540 nm branch terminated).

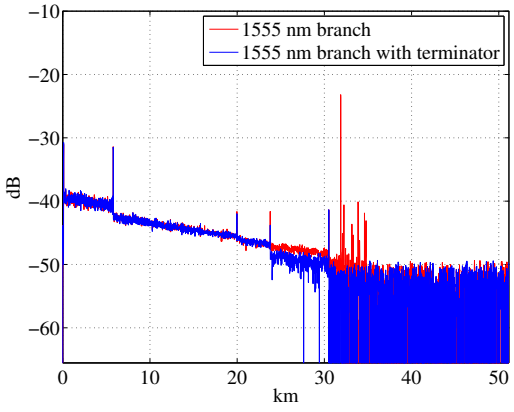

(f) 1555 nm branch (1555 nm branch terminated).

Figure 4.12: Configuration 5 traces.

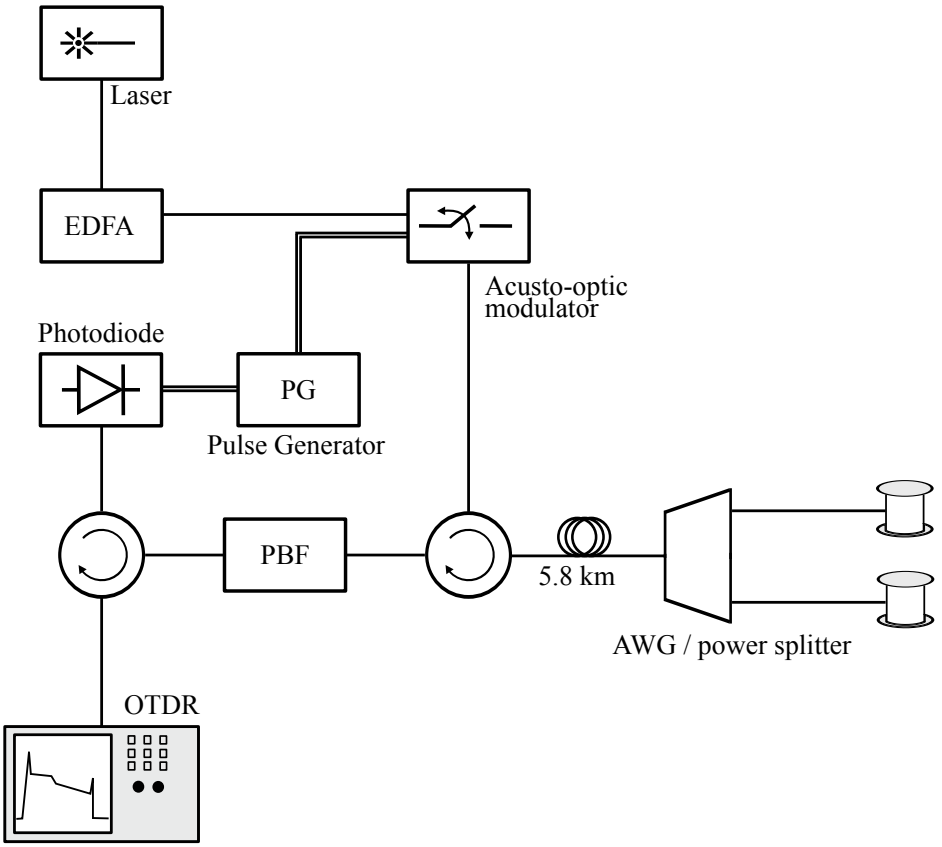

Figure 4.13: Modified monitoring scheme

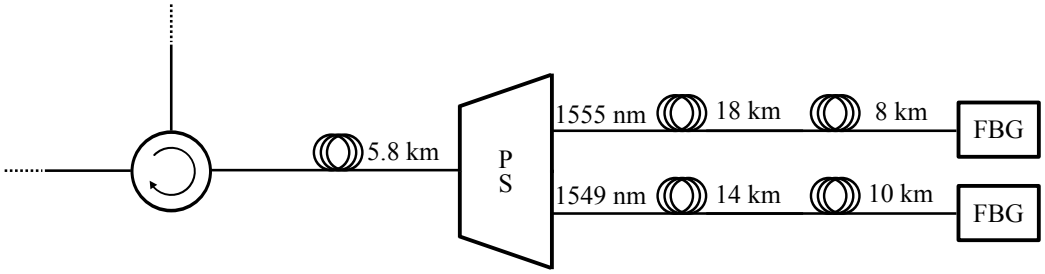

Figure 4.14: Configuration 6

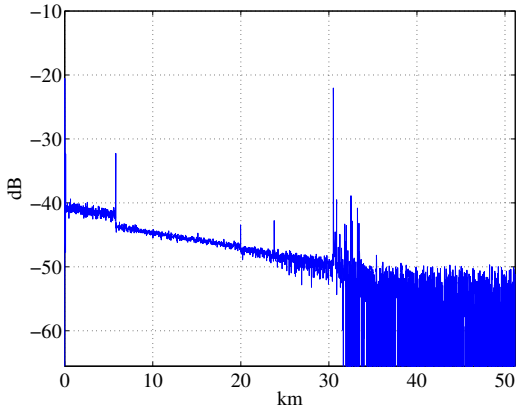

(a) 1549 nm branch.

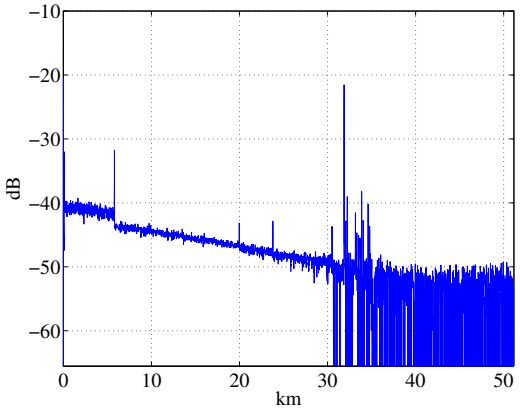

(b) 1555 nm branch.

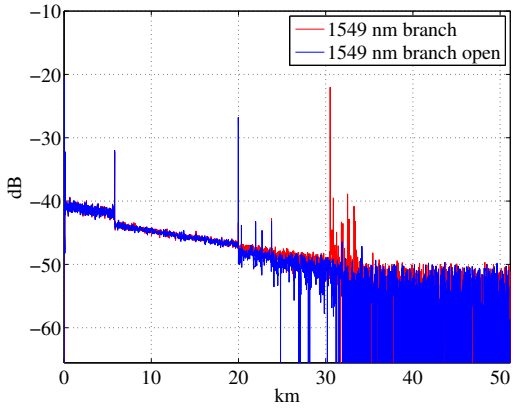

(c) 1549 nm branch (1549 nm branch open).

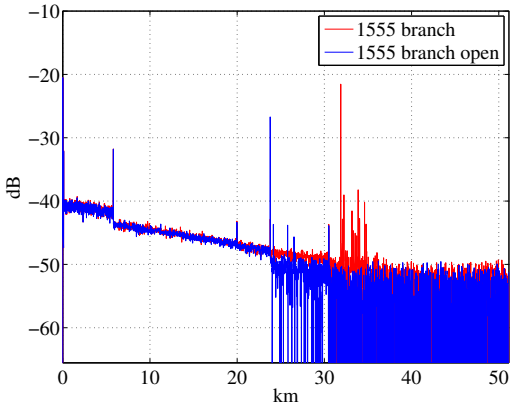

(d) 1555 nm branch (1555 nm branch open).

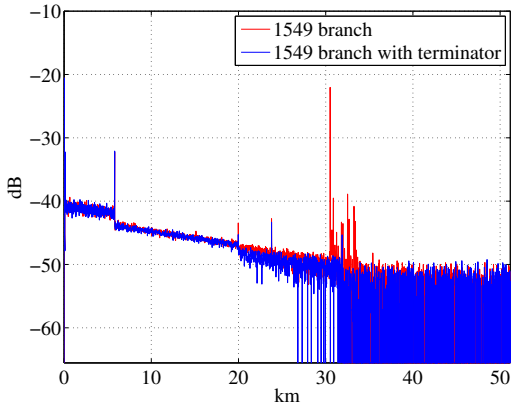

(e) 1549 nm branch (1549 nm branch terminated).

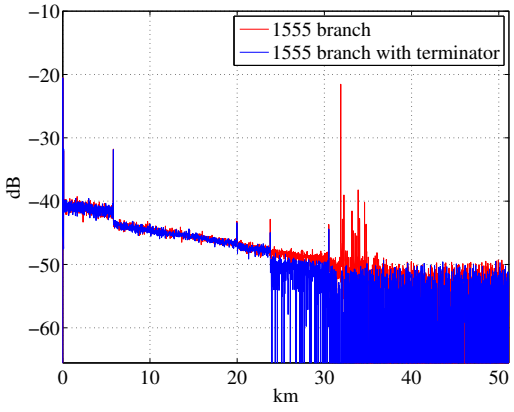

(f) 1555 nm branch (1555 nm branch terminated).

Figure 4.15: Configuration 6 traces.

Chapter 5

Conclusions and future work

The aim of this thesis was the implementation of an OTDR-based monitoring system for passive optical networks. In particular, I have considered TDM, WDM and TWDM passive optical networks as reference models. Two main link failures have been considered: a fiber break (reflective failure) and a fiber bend (or in general a non-reflective failure). First, the monitoring system has been realized and fully characterized. Then it has been tested using different configurations that simulate a remote note and several network branches.
The results show that if the remote node is implemented by an AWG, it's possible to identify the failure with a good precision both in presence of a fiber break and in presence of a non-reflective malfunctioning. Regarding the power splitter case, the results indicate that it's still possible identify link failures by observing the resulting traces, even if, with an high number of branches, it could be more difficult.
The future work should be oriented to testing the system in a real passive optical network, in particular with more realistic number of branches (up to 64), and implemented with R-SOAs as terminations, and by setting appropriate length to the link between the remote node (AWG or PS) and the ONU. Another important future work aspect consists in the realization of an automatic monitoring system in order to allow automatic (an possibly remote) network monitoring.

Appendix A

Pirelli© laser control with Matlab©

In the experimental setup I used a Pirelli© laser as optical source. The control software was implemented in Matlab©. The laser characteristic are summarized in table A.1.

Item	Min.	Typ.	Max	Unit
Tuning Range	-	39	-	nm
Frequency range (C-band)	191.15	-	196.25	THz
Channel Spacing	-	50	-	nm
Output Power	7	-	12	dBm
Spectral Linewidth	-	500	-	kHz

Table A.1: Pirelli© ITLA DTL-C13-050 characteristics.

The laser board is supplied with two voltages: 3.3 V and -5.2 V. The device and the computer communicate with RS-232 standard through serial port using a DE-9 connector, the details of the serial port settings are shown in table A.2. A Graphical User Interface (GUI) has been developed in order to simply the control of the laser. The GUI is proposed in figure A.2.

Setting	Value
Baud rate	9600
Data bits	8
Parity	none
Flow control	none
Stop bit	1

Table A.2: Serial port setting for computer-laser communication.

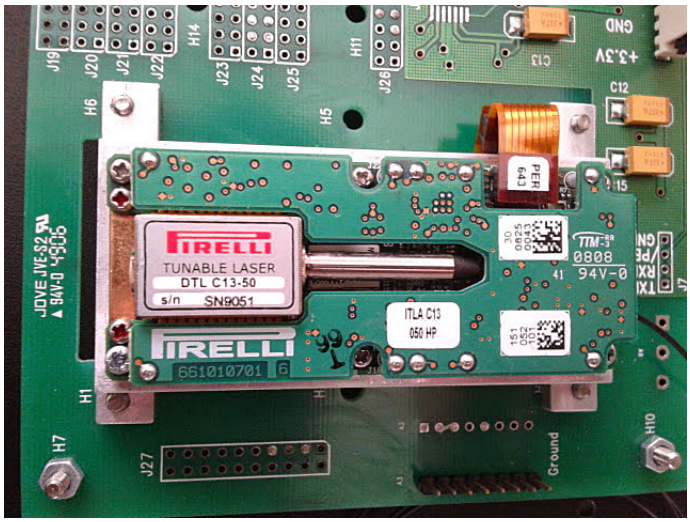

Figure A.1: Pirelli© ITLA DTL C13-050 laser.

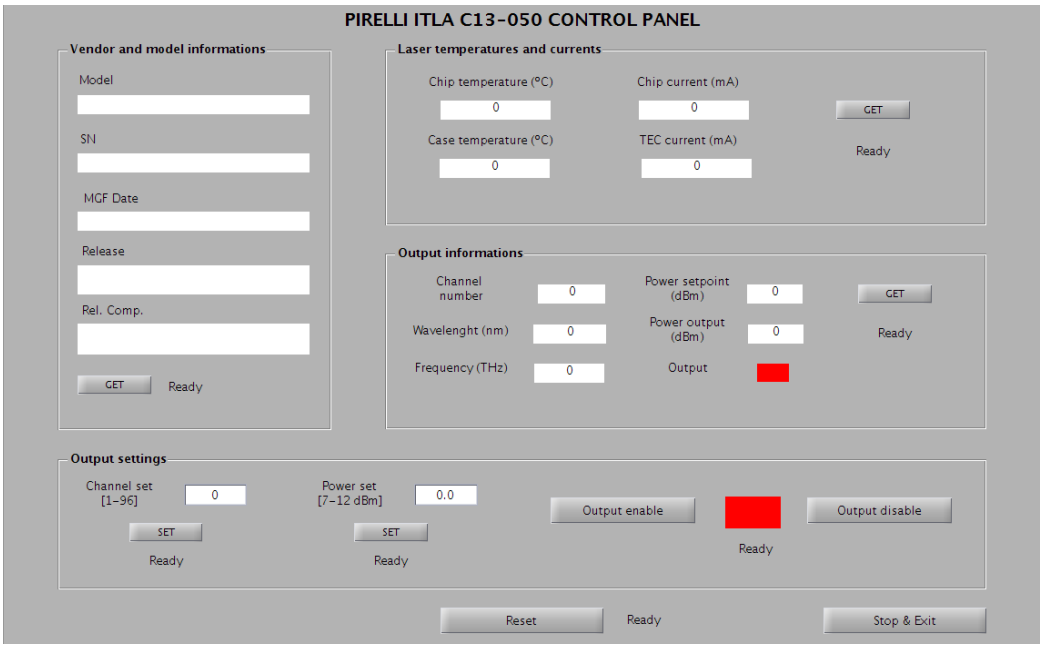

Figure A.2: Pirelli Laser Matlab© GUI.

A.1 Instructions set

The control software can send to the laser an instruction (e.g. to set a different channel) or a request (e.g. to get temperature information). The laser always replies communicating the result of the requested operation (successful or unsuccessful operation) or the requested data. All these instructions and replies are made up of 4 group of 8 bit (4 bytes). Typically the last two bytes are used to encode the particular information (e.g. the selected channel, the wavelength, etc..), and the first two bytes are used to identify the instruction. We will see the structure of each operation later. In what follows I use the decimal notation in order to represent the data exchanged between the laser and the control software, as in the following example:

$$\underbrace{10100100}_{164}\ \underbrace{01000001}_{65}\ \underbrace{00001101}_{13}\ \underbrace{10101100}_{172}$$

Information requests and instructions sent by the control software are:

- informations about the device: model, serial number, manufacturing date and release;
- informations about case and chip status: chip temperature, case temperature, chip current and TEC (thermoelectric cooler) current;
- output informations: channel number, power set point, output power, output frequency and output status (enabled or disabled);
- laser general state;
- channel set instruction;
- power set instruction;
- output enabling and disabling instructions;
- reset instruction.

Now I examine in detail each one of these operations, explaining in detail the sequence of request/reply messages and how the informations are encoded.

A.1.1 Device informations

These informations consist of: model, serial number, manufacturing date, release data. In this case all the informations sent by the laser are encoded in the last two bytes using the ASCII code, thus the laser can transmit two ASCII characters in a single reply. The protocol is the same for all the five informations and it works as follows:

1. the control software sends to the laser a request sequence which is different depending on the particular information requested (e.g. 48 3 0 0 for the model request) ;
2. the laser sends a reply sequence to inform that it's ready to transmit (also in this case the reply differs depending on the requested information);
3. the computer sends a special sequence that works like an acknowledgment: 176 11 0 0;
4. the laser transmits the data (two ASCII character in the last two bytes of the sequence);
5. for each received data sequence the control software sends an acknowledgment to the laser (176 11 0 0);
6. steps 4 and 5 continue until the laser receives the last acknowledgment;
7. the laser sends the end sequence: 244 11 0 0.

In table A.3 I report the particular sequences for the request and the corresponding laser reply.

Requested data	Request sequence	Reply sequence
Model	48 3 0 0	22 0 3 21
Serial number	64 4 0 0	150 4 0 11
MGF Date	80 5 0 0	246 5 0 12
Release	96 6 0 0	86 6 0 24

Table A.3: Device informations sequences.

From an implementation point of view, since the length of these information doesn't change, the control software can collect the ASCII characters sent by the laser, using a fixed number of cycles. In listing A.1, I show the code for the model request and the corresponding data collection.

Listing A.1: Model request.

```
% request starting
code0=[48 3 0 0];
fwrite(s, code0);
reply=fread(s,4);

% 1- get model name
code1=[176 11 0 0];
model='';
for i=1:10
    fwrite(s, code1);
    reply= fread(s,4);
    %temp=native2unicode(reply(3:4));
    temp=strcat(native2unicode(reply(3)),native2unicode(
       reply(4)));
    model=strcat(model,temp);
end
% request end
fwrite(s, code1);
reply= fread(s,4);
```

A.1.2 Case and chip status

The laser provides information about the status of the chip and the case of the laser itself, in particular: chip temperature, case temperature, chip current and TEC current. The protocol works as follows:

1. the control software sends a request string (208 88 0 0 for temperatures, 32 87 0 0 for currents);
2. the laser informs the control that it is ready to transmit (246 88 0 4 for temperatures, 6 87 0 4 for currents);
3. the control sends an acknowledgment string (176 11 0 0 as before);
4. the laser sends the chip temp sequence (or TEC current);
5. the control sends an acknowledgment;
6. the laser sends the case temp sequence (or chip current).

Temperature data have a precision of two decimal digits, current data have a precision of one decimal digits. In this case the currents and temperatures data are encoded using the binary representation of the last two bytes. The last two bytes must be concatenated, obtaining a 16-digit binary

string. This string is converted into a decimal value and it is divided by 10 or 100 according to the corresponding precision (i.e. if it is a current or a temperature data). The value of TEC current, instead, is encoded according to the two complement rule.

Listing A.2: Temperatures and currents request.

```
function [ chip_temp, case_temp, TEC_current, chip_current ] =
    get_laser_temp( s )
% PIRELLI ITLA C13-050 control software
% Get laser temperatures and currents informations.
% s= serial port object
% chip_temp = chip temperature
% case_temp =  case temperature
% TEC_current = thermoelectric cooler current
% chip_current = chip current

% temperature request
code0=[208 88 0 0];
fwrite(s, code0);
reply=fread(s,4);

% CHIP TEMP
code1=[176 11 0 0];
fwrite(s, code1);
reply= fread(s,4);
chip_temp_bin=strcat(dec2bin(reply(3),8), dec2bin(reply(4),8));
chip_temp= bin2dec(chip_temp_bin)/100;

% CASE TEMP
code1=[176 11 0 0];
fwrite(s, code1);
reply= fread(s,4);
case_temp_bin=strcat(dec2bin(reply(3),8), dec2bin(reply(4),8));
case_temp= bin2dec(case_temp_bin)/100;

% current request
code2=[32 87 0 0];
fwrite(s, code2);
reply=fread(s,4);

% TEC CURRENT
code1=[176 11 0 0];
fwrite(s, code1);
reply= fread(s,4);
TEC_current_bin=strcat(dec2bin(reply(3),8), dec2bin(reply(4),8))
    ;
TEC_current= two_complement(TEC_current_bin)/10;
```

```
if reply(3)>=128 %sign correction
    TEC_current= -TEC_current;
end

% CHIP CURRENT
code1=[176 11 0 0];
fwrite(s, code1);
reply= fread(s,4);
chip_current_bin=strcat(dec2bin(reply(3),8), dec2bin(reply(4),8)
   );
chip_current= bin2dec(chip_current_bin)/10;
end
```

A.1.3 Output informations

These are very important informations: output enable or disable, channel number, frequency output, power set point (specified by the user), and output power level. For each information, the control software sends a request string to which the laser replies with a single string. The frequency data is retrieved using two string, one for the integer part, and one for the decimal part. For the power level, the power set-point and the frequency output the encoding is the same as the previous case: the last two bytes must be concatenated, and converted into a decimal number to get the desired data. The laser doesn't provide the wavelength, it is simply obtained from the frequency. In the following table I summarize the request and reply strings.

Information	Request	Reply	Details
Output enable/disable	16 50 0 0	84 50 0 0	Output disable
		212 50 0 8	Output enable
Channel number	48 48 0 0	84 48 0 X	X = channel number
Frequency (integer part)	64 64 0 0	68 64 F_1 F_2	last two bytes encode the data
Frequency (decimal part)	64 64 0 0	164 65 C D	last two bytes encode the data
Power set-point	32 49 0 0	S 49 S_1 S_2	last two bytes encode the data
Power level	96 66 0 0	P 66 P_1 P_2	last two bytes encode the data

The value of S and P change according to the power set-point or the power level respectively but they are not useful for data decoding.

A.1.4 Laser general state

There is a particular request in the instruction set that allows to query the laser about the general status. If an error of any type occurs the laser com-

municates the malfunctioning sending a bad status reply. The particular query string is 0 0 0 0, if the the laser works properly the reply is 84 0 0 16.

A.1.5 Channel set

In order to set each one of the 96 available channels the control software sends a string with the following structure:

$$X \quad 48 \quad 0 \quad N$$

where N is the desired channel number and X is a number that is different for each channel. The number X associated with each channel is initialized into a matrix (the `ch_set_code` in listing A.3). Once the laser has successfully chanced the channel reply with a sequence with the following scheme:

$$Y \quad 48 \quad 0 \quad N$$

where N is again the channel number, and Y varies for each channel. This reply differs also in the case that the laser output is enable or not, so the easy way to check if the operation is correctly terminated consists in sending to the laser the query string about the actual channel number.

Listing A.3: Channel set.

```
function [check]= set_channel(s, ch_number)
% PIRELLI ITLA C13-050 control software
% Set the laser channel
% s = serial port object
% ch_number = selected cheannel (by the user)
% check= control variable that indicates a successfull/
   unsuccessfull operation

global ch_set_code;
% global ch_reply_code;

% check if a valid channel is selected
if ch_number<1 || ch_number>96
    check=0;
    return
end

% generate the instruction for the corresponding channel
code0=[ch_set_code(ch_number); 48; 0; ch_number];
fwrite(s, code0);
reply=fread(s,4);
```

```
% channel number request
code1=[48 48 0 0];
fwrite(s, code1);
ch_number_reply=fread(s,4);
ch_num_laser=ch_number_reply(4);

% check if the selected channel was setted properly (query to
   the laser)
if ch_num_laser==ch_number
    check=1; % success
else
    check=0;
end

end
```

A.1.6 Power set

Allowed power level from the laser are values from 7 dBm to 13 dBm with a resolution of 0.1 dBm, so there are 61 possible power levels. The power set instruction has the same scheme of the channel set command. The power level specified by the user is encoded in binary format using 16 bits, that are placed in the last two bytes of the request string. The request string is in the form:

$$A \quad 49 \quad B \quad C$$

where A is a number which changes according to the power level, and B and C are the result of the power level encoding. The laser reply with a confirmation sequence with structure:

$$D \quad 49 \quad B \quad C$$

where B and C are the same as the request string, and D is again a special number that depends on the particular selected power level. In this case too, the numbers A and D are stored in matrices (`power_set_code` and `power_reply_code` in listing A.4) initialized during the GUI initialization.

Listing A.4: Power set.

```
function [ check ] = set_power( s, power )
% PIRELLI ITLA C13-050 control software
% Set the laser output power
% s = serial port object
```

```
% power = selected power level (by the user), only one decimal
   number is
% allowed
% check= control variable that indicates a successfull/
   unsuccessfull operation
global power_set_code;
global power_reply_code;

% check power level
if power>13 || power<7
    check=0;
    return;
end

% generate the instruction for the corresponding power level
a=power_set_code( round(power*10)-69 );
power_bin = dec2bin( round(power*100) , 16);
b=bin2dec(power_bin(1:8));
c=bin2dec(power_bin(9:end));
code0=[a 49 b c];
fwrite(s, code0);
reply=fread(s,4);

% generate the instruction for the corresponding laser reply
d=power_reply_code(fix(power*10)-69);
code1=[d; 49; b; c];

%compare the reply with expected one
if reply==code1
    check=1; % success
else
    check=0;
end


end
```

A.1.7 Enabling and disabling output

These are the most important instructions, also for security motivations. The protocol is very simple in this case too. The control software sends the laser the output enable instruction: 129 50 0 8. Then it sends the instruction 0 0 0 0 in order to get the laser state, if the laser doesn't signal any problem the operation is successful terminated. The same procedure is adopted for disable the output, with the only difference that the output disable instruction is: 1 50 0 0.

Listing A.5: Output enabling function.

```
function [ check ] = enable_output( s )
% PIRELLI ITLA C13-050 control software
% this function enable the laser output.
% s = serial port object
% check= control variable that indicates a successfull/
   unsuccessfull operation

% output enable instruction
code=[129 50 0 8];
fwrite(s, code);
reply=fread(s,4);

% check the state of the laser
code0=[0 0 0 0];
fwrite(s, code0);
reply=fread(s,4);

while reply~=[84; 0; 0; 16]
    fwrite(s, code0);
    reply=fread(s,4);
end
check=1;

end
```

Listing A.6: Output disabling function.

```
function [ check ] = disable_output( s )

% PIRELLI ITLA C13-050 control software
% this function disable the laser output.
% s is a serial port object (connected to the laser)
% check= control variable that indicates a successfull/
   unsuccessfull operation

% control variable, if the operation is successfull
% is set to one.
check=0;

% output disable instruction
code=[1 50 0 0];
fwrite(s, code);
reply=fread(s,4);

% check the state of the laser
code0=[0 0 0 0];
```

```
fwrite(s, code0);
reply=fread(s,4);

if reply==[84; 0; 0; 16]
    check=1; % success
end

end
```

Bibliography

[1] Govind Agrawal, *Nonlinear Fiber Optics*, Academic Press, 2013.

[2] Nirwan Ansari, Jingjing Zhang, *Media Access Control and Resource Allocation For Next Generation Passive Optical Networks*, Springer, 2007.

[3] Cedric F. Lam, *Passive Optical Networks, Principles and Practice*, Academic Press, 2007.

[4] Yuanqiu Luo, Xiaoping Zhou, Frank Effenberger, Xuejin Yan, Guikai Peng, Yinbo Qian and Yiran Ma, *Time- and Wavelength-Division Multiplexed Passive Optical Network (TWDM-PON) for Next-Generation PON Stage 2 (NG-PON2)*, Journal of Lightwave Technology, Vol. 31, No. 4, 2013.

[5] Leonid G. Kazovsky, Wei-Tao Shaw, David Gutierrez, Ning Cheng, and Shing-Wa Wong, *Next-Generation Optical Access Networks*, Journal of Lightwave Technology, Vol. 25, No. 11, 2007

[6] Marco Leo and Mariangela Trotta, *Performance evaluation of WDM-PON RSOA based solutions in NGAN scenario*, ITCE Congress, 2011.

[7] Luca Palmieri, *Slide del corso Sistemi in fibra ottica e laboratorio*, 2013.

[8] Guido Maier, *Introduzione alle Passive Optical Network*, 2010.